# COMMUNICATION NETWORK OPTIMIZATION VIA WIRELESS CHANNEL MODELLING AND MEAN FIELD GAME THEORY

*Nicholas Destounis*

Department of Electrical & Computer Engineering

McGill University

Montreal, Canada

August 2016

---

A thesis submitted to McGill University in partial fulfilment of the requirements of the degree of Master of Engineering.

# ABSTRACT

This thesis focuses on channel modelling and the applications of Mean Field Game (MFG) theory to cellphone communication systems.

First, it proposes a new continuous time state-space stochastic channel model which combines the effects of long-term and short-term fading in order to describe the input and output signal power of the wireless channel.

Then, second, the new channel model and MFG theory are applied to the problem of decentralized uplink power control in Code Division Multiple Access (CDMA) cellphone networks. In this problem, the user devices are competing with each other by dynamically controlling their transmit power, as well as their position in space in a second problem, in order to maximize individual quality of service (QoS) while minimizing individual control costs.

The third part of this thesis provides a dynamic system model of Orthogonal Frequency Division Multiple Access (OFDMA) femtocell systems in continuous time; it then gives a formulation of a downlink power control problem for competing femtocell base stations in a dynamic game setting which is solved using MFG theory.

In this work nonlinear MFG theory is used in order to solve for Nash Equilibrium strategies of the decentralized CDMA and OFDMA control problems, to be specific it employs numerical methods for the solutions of the Hamilton-Jacobi-Bellman and McKean-Vlasov-Fokker-Planck-Kolmogorov equations of MFG theory. Illustrative solutions and simulation examples are then presented.

# RÉSUMÉ

Cette thèse porte sur la modélisation des canaux sans fil et les applications de la théorie des jeux à champ moyen aux systèmes de communication de téléphones cellulaires.

Premièrement, on propose un nouveau modèle stochastique de canaux sans fil à espace d'états en temps continu qui combine les effets d'atténuation à long terme et ceux à court terme pour décrire la puissance d'émission d'entrée et de sortie d'un signal qui traverse le canal sans fil.

Deuxièmement, le modèle et la théorie des jeux à champ moyen sont appliqués au problème de contrôle de puissance d'émission décentralisé de liaison montante dans les réseaux de téléphones cellulaires «Code Division Multiple Access» (CDMA). Dans ce problème, les utilisateurs sont en concurrence les uns contre les autres et contrôlent leur puissance d'émission. Dans un deuxième problème, la position dans l'espace est aussi contrôlée. Ceci a pour but de maximiser leur qualité de service et de minimiser leurs coûts de contrôle individuels.

La troisième partie de cette thèse fournit un modèle dynamique des systèmes de femtocellules «Orthogonal Frequency Division Multiple Access» (OFDMA) en temps continu. On formule ensuite un problème de contrôle de puissance d'émission de liaison descendante comme jeu dynamique où les joueurs en concurrence sont les femtocellules.

Une partie importante du travail présenté dans cette thèse est basée sur la théorie non linéaire des jeux à champ moyen qui est utilisé afin de trouver des stratégies

d'équilibre de Nash des problèmes de contrôle CDMA et OFDMA décentralisées. Précisément, on utilise des méthodes numériques pour résoudre les équations Hamilton-Jacobi-Bellman et McKean-Vlasov-Fokker-Planck-Kolmogorov de la théorie des jeux à champ moyen. Des solutions illustratives et des exemples de simulation sont finalement présentés.

# ACKNOWLEDGEMENTS

I first want to express my utmost gratitude to my supervisor Professor Peter E. Caines for his invaluable research insight and for his close guidance throughout the entirety of my Masters studies. He is a brilliant teacher and scholar from whom I learnt immensely many things. I am very grateful for his encouragement, enthusiasm, generosity, and for his incredible patience. Researching under his supervision has truly been one of the most enlightening experiences in my life and I am very fortunate to have had the opportunity. I importantly thank him for helping prepare this thesis with his constructive feedback. I also want to thank him for our very many enjoyable conversations about music, even in the busiest of times.

I want to thank Professor Aditya Mahajan for our conversations and especially for all the academic and career advice. I also thank Professor Benoit Champagne for lending his expertise on communication systems with his very educational input on the communications aspects of our research.

I am most grateful for the financial support provided by NSERC, FRQNT and Hydro-Québec.

I would also like to thank my friends and colleagues Maxime, Mohammad, Dena, Ali, Jayakumar, Hamed, Jalal, Jhelum, Mohamad, Shuang, Mohamed and Nevroz for their help and for all the laughs, making my studies all the more enjoyable.

I most importantly want to thank my parents and my sister Liz for their unconditional love and their support in everything I do in my life, without which none of my accomplishments would be possible. It is to them that this thesis is dedicated.

# Contents

# LIST OF FIGURES

# LIST OF TABLES

# Chapter 1

# Introduction and Background

## 1.1 Introduction

Optimization in cellphone networks has become an important topic in present day engineering. With the emergence of smart-phones, cellphone devices are moving towards becoming all purpose computing machines. A great deal of research is presently pursuing pushing cellphone networks towards more robust and efficient designs which are self-organized to as great an extent possible [5, 6]. These networks must be designed in order to provide an acceptable rate of communication between user devices and network base stations. This is especially important due to the presently increasing amounts of data being exchanged through various cellphone media applications. Therefore, because the effective wireless transmission between devices and the central network is an important design consideration, the discussion of energy efficiency and quality of service (QoS) remain two important aspects of these networks when it comes to planning future generation technologies [6].

In Code Division Multiple Access (CDMA) and Orthogonal Frequency Division Multiple Access (OFDMA) based cellphone communication systems the topics of power control and (in the latter case) frequency resource allocation are of great importance. In addition, due to the emergence of low-power base stations called femtocells which are increasing in number in office spaces, public places and user homes, these topics have encountered new complexities. The coordination of these devices is not a trivial task due to the unpredictable nature of their installation within the network as well as the difficulty of centrally controlling their operation [5].

At the level of communication between user devices and base stations in these CDMA and OFDMA cellphone systems, efficient operation presents many challenges, two of which are examined in this work: firstly, the accurate mathematical modelling of the physical phenomena present in the system, especially the wireless channel carrying the information and secondly, the efficient design of robust and scalable algorithms for the operation of devices in terms of their transmit power control. Both of these problems are central in developing power control solutions which aim to provide adequate QoS while also using as little power as possible for signal transmission, an important goal for any given user and a central topic in this work.

## 1.2 Quality of Service

An important metric for QoS in wireless communication is the signal-to-interference-plus-noise-ratio (SINR). Consider a shared wireless channel being accessed by $N$ different devices simultaneously. The SINR of a transmitting pair $i$ (transmitter and receiver) in the wireless channel can be expressed by $\gamma_i$ in the following equation

$$\gamma_i = \frac{h_i p_i}{\rho(N) \sum_{j=1, j\neq i}^{N} h_j p_j + \eta} \tag{1.1}$$

where $p_i$ is the transmit power of transmitter $i$, $h_i$ is the channel gain coefficient of transmitter $i$ and $\rho(N)$ is a function of number of transmitting devices $N$ in the wireless system and depends on the multiple access protocol. For CDMA systems with non-orthogonal codes, the standard result is that $\rho(N) = \frac{1}{N}$ but for the transmission on a particular frequency band in OFDMA, the function $\rho(N)$ is equal to one.

The importance of the SINR in communication can best be described through the Shannon-Hartley Theorem [7] where it is stated that the channel capacity $C$, or tightest upper bound on the information rate of the channel, is given by the following expression.

$$C = Blog_2(1 + \gamma_i) \tag{1.2}$$

where B is the bandwidth of the channel. Therefore, a natural choice of QoS metric is given by the SINR, especially in contemporary networks where the channel capacity is being used to its limit and therefore a higher SINR would correspond to a higher data throughput [6].

## 1.3 Wireless Channel Modelling

Accurate wireless channel modelling is an important problem when considering wireless network optimization problems. In general, the modelling of a wireless channel considers various physical phenomena which result in mathematical models ranging from low level specific descriptions to very high level approximations. Correspondingly, as described in [1], wireless channel models come in a variety of forms, the usefulness and accuracy of which depend greatly on the application of interest. Wireless channel models are sometimes deterministic and sometimes described in terms of statistical behaviour. Some models account for frequency specific behaviour and other times are assumed to be frequency independent, the latter case being referred to as flat-fading channels. Again depending on the application, some models include considerations of Doppler effects while others do not.

Traditional channel models used in the literature to describe the wireless channel at the high level include models of path loss, long-term fading (also known as shadowing or shadow fading) and short-term fading (also known as scattering). Each of these processes describe power variations of a transmitted signal as it travels through a lossy wireless channel while also being influenced by the relative motion between the transmitting device and the receiving device. For example, a cellphone user travelling around a city in a vehicle will encounter various obstacles and physical disturbances influencing the power of the received signal from his cellphone device to the local macrocell base station. An illustrative graph of the effects of these three important channel attenuation processes is shown in Fig. 1.1 where the channel power gain of a given wireless channel is compared over increasing distances on the log scale.

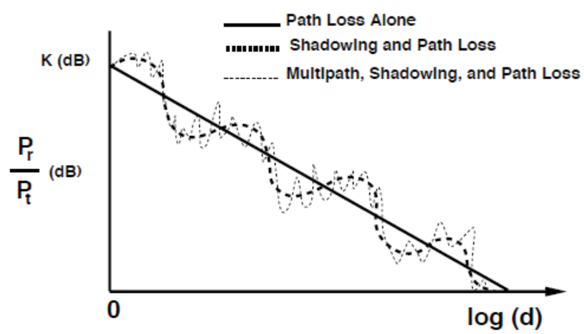


**Fig. 1.1** Path loss, long-term fading and short-term fading versus distance taken from [1]

As is depicted in Fig. 1.1, path loss describes a deterministic linear drop in signal power (in dB) as the logarithm of the channel distance increases. This phenomenon can be explained by the fact that an electromagnetic wave will experience loss in energy as it travels through a wireless medium (such as air) due to (i) the dissipation of power radiated by the transmitter (in an inverse square relationship) and (ii) the effects of the channel medium [1]. On the Watts scale, a simple path loss model describes the channel power gain using the following equation [1]

$$P_r = P_t \left( \frac{\lambda}{4\pi d_0} \right)^2 \left( \frac{d_0}{d} \right)^\gamma \tag{1.3}$$

where $P_r$, $P_t$ are the channel output and input power respectively, $d$ is the distance between the transmitter and receiver, $d_0$ is a reference distance, $\lambda$ is the signal wavelength and $\gamma$ is the path loss exponent. On the decibel scale, the gain is expressed as follows

$$P_r(dBm) = P_t(dBm) - 20log_{10}(4\pi d_0/\lambda) - 10\gamma log_{10}(d/d_0) \tag{1.4}$$

which describes the linear drop in channel received power as the log distance increases.

Complementing path loss, long-term fading describes an additional channel attenuation effect due to large scale random phenomena. These large scale phenomena correspond to the transmitted signal reflecting off of objects as it travels through the medium, losing power at every bounce. In a static setting, the channel gain of a long-term fading channel is frequently modeled to be a log-normal random variable. The probability density function of a log-normal random variable can be found in Appendix A. Long-term fading typically occurs in the time scale of seconds [8].

Furthermore, the effects of short-term fading on the channel due to signal scattering introduce another smaller scale random fluctuation of power attenuation. As is indicated by the name, scattering corresponds to the electromagnetic wave splitting up into many plane waves which undergo different phase shifts and power losses and which finally add up at the receiver. The output signal magnitude (envelope) of a short-term fading channel is frequently modelled to be a Rayleigh random variable [1] in the case where it is assumed that there is an absence of a direct line of sight (LOS) component of the transmitted signal reaching the receiver. Otherwise, the output signal envelope is frequently modelled to be a Rician random variable [1]. The probability density functions of Rayleigh and Rician random variables can be found in Appendix A. Short-term fading typically occurs in the time scale of milliseconds, significantly faster than the effects of long-term fading [8].

In a dynamic setting, a very popular discrete time modelling approach in literature is to model the random attenuation processes, namely those of long-term and short-term fading to be i.i.d. by claiming that their time evolution is extremely chaotic. Effectively, one would therefore model long-term fading to be i.i.d. log-normal and short-term fading to be i.i.d. Rayleigh or Rician in the non-LOS and LOS cases respectively. Though this approach simplifies analysis, the clear drawback is that previous information of the channel becomes irrelevant where in some situations in real physical systems, this is not entirely accurate. A solution to this issue is the use of continuous-time state-space generalized models of the three important attenuation phenomena which will be discussed in Chapter 2.

This work focuses mainly on flat-fading wireless channels at the high level and specifically uses modelling approaches having the main goal of providing an input output relationship of the channel describing the power of a signal travelling through the channel from the transmitter (input) to the receiver (output). Doppler effects are also ignored. The models described and developed in this work include the effects of path loss, log-normal long-term fading and Rayleigh short-term fading in both the traditional case and in terms of generalized continuous-time models which are to be presented in future chapters of the work.

## 1.4 Mean Field Game Theory for Nonlinear Stochastic Dynamical Systems

Mean Field Game (MFG) theory studies large population, dynamical, multi-agent, competitive systems. In particular, it studies existence of Nash equilibria and the strategies of individual agents which generate these equilibria by exploiting the relationship between finite and infinite population problems. The theory originated in the work of Huang et al. in [9, 10, 11] and also independently in the work of Lasry and Lions in [12, 13, 14]. An overview basic MFG theory is now introduced, referring to [15]. It is remarked that the literature contains developments of the more general definitions and framework of MFG theory including broader application ranges. The introduction and overview given in this work corresponds only to the base framework which is of interest in the particular applications considered in this work.

One of the key results of MFG theory is that, in the infinite population limit, individual agent feedback strategies exist for which any agent is in a Nash equilibrium with respect to a mass or Mean Field, for which the behaviour is pre-computable. This Mean Field is in turn generated by the collective behaviour of all agents in the system where each agent is asymptotically negligible in the infinite population limit. Each agent in the system consequently becomes a generic agent following the same homogeneous dynamics and considering the same cost function where the dynamics and cost of the generic agent are linked by the Mean Field. In addition, the optimal controls found in the infinite population approximation of the system result in an approximate Nash or $\epsilon$-Nash equilibrium control set if applied in the finite population system where $\epsilon$ approaches zero as the number of agents in the system approaches infinity.

In MFG theory a key feature is that the dynamics of the Mean Field density (assumed to exist), the value function of the generic agent and the best response controls of the generic agent correspond to the solutions of a MFG Fokker-Planck-Kolmogorov equation (equivalently a McKean Vlasov SDE), and a MFG Hamilton-Jacobi-Bellman equation of the generic agent which are linked by the Mean Field. In nonlinear MFG theory in particular, the work in [16] describes a solution methodology to a loop relation of these MFG PDEs using a contraction argument which lends itself to the use of numerical methods in order to approximately solve these equations which is of importance in this work.

## 1.5 Decentralized Stochastic Control in CDMA Cellphone Networks Using Mean Field Game Theory

The problem of dynamic CDMA cellphone network optimization in a competitive setting using MFG theory, where the user devices become intelligent competitive agents, has been discussed in the literature. In fact, the original motivating problem for the development of MFG theory was the formulation of a centralized CDMA stochastic control problem which lead to theoretical developments resulting in one of the first MFG theory papers [9].

Since then the more recent work [17, 18] has investigated the application of MFG theory to CDMA network optimization from a different perspective, where the authors provide an analysis of as well as a computational methodology for the optimal (in the sense of infinite population Nash equilibria) feedback controls of each transmitting agent in the system by solving the nonlinear Mean Field equation loop consisting of a Hamilton-Jacobi-Bellman equation (HJB), a Fokker-Planck-Kolmogorov (FPK) equation and a best response control for the generic agent. Building on this work, some of the work in this thesis follows similar computational methods for the solution of new communications optimization problems as well as an extended CDMA MFG optimization problem using more elaborate channel modeling techniques.

## 1.6 Heterogeneous Networks and OFDMA Communication

Heterogeneous Networks (HetNets) is a term which has recently been used to characterize contemporary Fourth Generation (4G) standard cellphone networks. A main point of discussion concerning these contemporary cellphone networks is the managing of interference in the presence of multiple heterogeneous tiers (hence the term HetNet) of base stations called picocells and femtocells which are operated in a decentralized manner [5] in the area of the main base station called the macrocell. An illustration of a network consisting of multiple small cells within a given macrocell radius is given in Fig. 1.2.

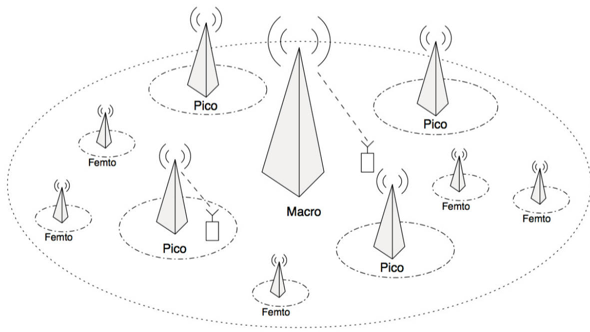


**Fig. 1.2** Illustration of a single macrocell multi-tier network with picocells and femtocells taken from [2]

In addition to the picocells, which are network operated and essentially act as lower power macrocells, user operated femtocells connected to the network via wired backhaul are becoming extremely popular solutions for transmit power reduction of devices in indoor areas such as office buildings and malls [5]. As these femtocells are becoming increasingly popular the necessary interference management techniques become increasingly important [6]. In particular, due to the unplanned and highly unpredictable installation and operation of these femtocells from the central network's point of view, decentralized solutions are natural in this setup [5, 6]. To illustrate the irregularly distributed nature of these networks, Fig. 1.3 shows a two-dimensional geographical picture of a real femtocell (two tier) network where the red and blue dots are macrocell and femtocell base stations respectively. It is observed that within a given macrocell radius, the femtocell placements are highly irregular.

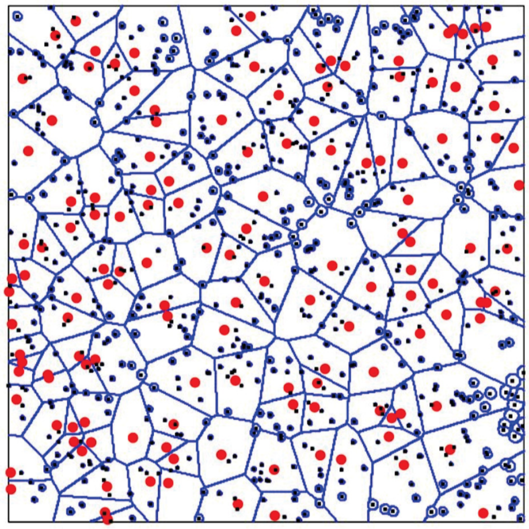

**Fig. 1.3** Example map of a real two tier network taken from [2]

The main realization of the 4G standard is the Long Term Evolution Advanced (LTE-A) [19, 20, 21] network technology. These heterogeneous networks mainly use this technology which uses OFDMA (or its variants) as the main protocol for multiple access within each cell. OFDMA is a multiple access protocol which divides frequency and time resources into multiple resource blocks which are each allocated to a user device. The communication bandwidth is divided evenly into orthogonal slices and time is similarly divided into slots which, together, result in a grid of blocks in the frequency-time plane as seen in Fig. 1.4. During each time slot, each given frequency slice is allocated by the base station to at most one of its user devices for communication. Fig. 1.4 shows an example of allocated resource blocks to various user devices as time evolves. Given this set-up, the decision makers (the base stations) in an OFDMA communication system have, at the highest level, a two fold decision process to solve. First, it must be decided which frequency blocks are associated to each user during any given time step. Second, the transmit power over each of the resource blocks has to also be allocated and adjusted (controlled) in an efficient manner. Each femtocell base station should also have an understanding of its neighbours' behaviour as well as the behaviour of the macrocell in order to

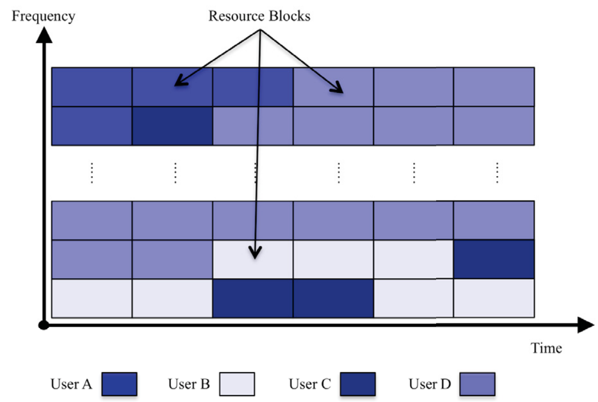


**Fig. 1.4** Allocation of resource blocks to various users in the LTE time-frequency grid taken from [3]

allocate frequency resources and control transmit powers to the benefit of its own user devices. Hence, competition can be seen as a natural aspect of this network problem because each small cell is in competition with other small cells in order to provide a good level of QoS to its users. This competition arises naturally from the interference within each band, where it is of importance to note that interference across different bands is not present due to the orthogonality of the sub-bands.

OFDMA femtocell optimization problems have become extremely popular in the literature due to the increasing use of femtocells. There are many different approaches used in order to solve the frequency resource and power allocation problems in both the uplink and downlink. In [22] the authors apply a game theoretic approach, solving a downlink power allocation problem by modelling the system as a Stackelberg game and allocating power using what is called the Water Filling algorithm. The work of [23] considers the joint problem of downlink admission control and power allocation and provides a Nash Equilibrium solution amongst the femtocells. In [24] the problem of downlink power control is examined using Robust Stackelberg Equilibria using a similar approach to [22]. In [25] a new algorithm for decentralized spectrum allocation is presented in a static setting using randomization.

One of the main features of the works described above, as well as a large portion of related work, is that they approach the problem of resource allocation and power allocation at each time step as a static optimization problem with little or no mention of modelling of system or agent dynamics. They do not fully consider the dynamics of femtocell systems by including the dynamics of channel behaviour and the dynamics of other agents in the system. Furthermore, in literature in general, there is very little work which considers dynamic optimization or stochastic optimal control of such competitive decentralized networks, for example in the context of a dynamic game.

## 1.7 Thesis Scope, Organization and Contributions

This thesis focuses first on wireless channel modelling and then uses the resultant models in an application of MFG theory to cellphone communication systems. The thesis is organized as follows.

Chapter 2 presents a novel continuous time state space channel model which combines the effects of path loss, long-term fading, and short-term fading into a concatenated nonlinear model which, in its entirety, provides a relationship between the signal power at the input (transmitter) and output (receiver) of the channel. The model is then analysed and illustrated through simulations.

Chapter 3 builds upon the work of [17, 18] and presents an application of MFG theory and the novel channel model derived in Chapter 2 to two related CDMA cellphone optimization problems where agents are applying decentralized control of transmit power to minimize their personal costs which correspond to a linear combination of QoS and transmit power over time. In the first application the agents are static but in the second they each have a certain specified controllable mobility in space.

Chapter 4 presents numerical algorithms for the solution of each of the two CDMA optimization problems and generates illustrative solutions and simulation examples.

Chapter 5 proposes the modelling of OFDMA femtocell systems as a continuous time dynamic stochastic game where the agents, here being the femtocells, are dynamically controlling their power in each frequency band in a decentralized manner while competing with all other femtocells in order to minimize their own costs; as in the case of the CDMA problems discussed in Chapter 3 these costs correspond to a linear combination of QoS and transmit power. It then employs MFG theory and numerical methods are used for (i) the solution of the corresponding MFG PDEs and (ii) agent state sample paths providing illustrative simulation examples.

Chapter 6 summarizes with a conclusion and discusses potential extensions of the work.

It is emphasized that in this work all optimal solutions are to be interpreted in the sense of Nash Equilibria (generated by agent best responses), and that this holds whether user devices on a CDMA network or femtocell base stations in an OFDMA system are under consideration.

# Chapter 2

# Stochastic Dynamic Wireless Channel Models

## 2.1 Overview

This chapter proposes a novel wireless channel model by combining the wireless channel attenuation phenomena of path loss, long-term and short-term fading. This is done in order to provide an accurate relationship between the power of a transmitted signal at the channel input and the corresponding output signal power of a signal reaching the receiver after passing through the wireless channel. To be specific, the model in this work combines continuous-time state space stochastic differential equation (SDE) models for (i) log-normal long-term fading and (ii) Rayleigh short-term fading effects in order to provide a combined concatenated long-term and short-term fading model; these models were initially considered separately in [4, 26, 27, 28, 29] and are briefly summarized in Section 2.2.

In this work, the terms "long-term" and "short-term" fading correspond to the large and small scale variations of signal power due to the movement of transmitting devices. The words "long-term" and "short-term" imply the distinction of different time scales but can equivalently be understood to be a distinction of long and short distances. This is due to the general understanding that a transmitting device takes longer to travel further distances (assuming almost constant velocity). The abstraction of the notion of distance into an analogous (in this case) notion of time is a standard methodology in wireless channel modelling as described in [1] and is used in this work.

## 2.2 SDE Wireless Channel Models

The work in [4, 26, 27, 28, 29] describes continuous-time state-space dynamic generalizations of traditional channel models, in particular those of log-normal and Rayleigh fading. The state-space models were all developed to take account of continuous random dynamics which are not described by the traditional models while also remaining consistent with these traditional models at the macroscopic level. In a dynamic setting, instead of assuming the independence in time of the random channel attenuation phenomena, these models offer transition densities on the continuous time scale.

### 2.2.1 Long-term Fading

Traditional models of long-term fading use the log-normal distribution in order to model the signal power attenuation due to long-term fading and path loss. A signal travelling from the transmitter to the local area of receiver will experience multiple reflections off objects in its path. Each reflection results in some power loss of the incoming signal as some of the energy is absorbed by the obstacle. This power loss occurs in a multiplicative manner at each obstacle. Therefore, on the decibel scale, the power loss will be an additive loss.

Because the power lost at each reflection is best described by a random quantity due to the potential chaotic behaviour of the channel, and by virtue of the Central Limit Theorem, the sum of power losses, on the decibel scale, due to every obstacle on the path from transmitter to receiver is frequently be modelled to be a Gaussian distributed random variable. Going back to the Watts scale, this power attenuation is modelled as being log-normal.

In a dynamic setting, one typically models the channel gain due to long-term fading at any time $t$ as the exponential $e^{X_t}$ where $X_t$ is a sequence of i.i.d. Gaussian random variables distributed with mean equal to the deterministic path loss given the distance between transmitter and receiver. Instead, the models developed in [4, 26, 29] consider the long-term fading channel gain to be given by $e^{\beta(t)}$ where now $\beta(t)$ is a continuous-time stochastic process following the first order linear SDE

$$d\beta(t) = -a(\beta(t) + b)dt + \sigma_\beta dW_\beta(t), \quad \beta(0) = \beta_0, \quad t \in \mathbb{R}_+, \tag{2.1}$$

where $a > 0$, $b > 0$, $\sigma_\beta > 0$ and $W_\beta(t)$ is a standard Wiener process. Here the parameter $-b$ is the long-term mean towards which $\beta(t)$ is tracking corresponding physically to the path-loss exponent; the parameter $a$ is a rate of adjustment towards the long-term mean $-b$; the parameter $\sigma_\beta$ tunes the variance of the diffusion term of $\beta(t)$ and depends on the intensity of random phenomena causing the long-term fading effects such as the presence of obstacles and transmitter movement. If the initial condition $\beta_0$ is Gaussian distributed, then $\beta(t)$ will remain Gaussian distributed [4]. On the macroscopic level, the model remains consistent with the traditional log-normal model because the effective channel power gain, $e^{\beta(t)}$ will be log-normally distributed at any time $t$.

### 2.2.2 Short-term Fading

Traditional Rayleigh short-term fading models use the Rayleigh distribution to model the output signal envelope of the short-term fading channel. Rayleigh fading is a result of local area signal scattering whereby a transmitted signal scatters into $N$ plane waves with different phase shifts and envelopes which add up at the receiver.

Let the $n$-th plane wave (after scattering) be given by the equation

$$E_n(t) = I_n(t)\cos(\omega_c t) - Q_n(t)\sin(\omega_c t), \qquad t \in \mathbb{R}_+, \tag{2.2}$$

where $\omega_c$ is the carrier frequency and $I_n(t)$ and $Q_n(t)$ are the in-phase and quadrature components of the signal given by

$$I_n(t) = \sum_{m=1}^{N} r_{n,m}\cos(\omega_{n,m}t + \theta_{n,m}), \qquad t \in \mathbb{R}_+, \tag{2.3}$$

$$Q_n(t) = \sum_{m=1}^{N} r_{n,m}\sin(\omega_{n,m}t + \theta_{n,m}), \qquad t \in \mathbb{R}_+, \tag{2.4}$$

where $\omega_{n,m}$, $\theta_{n,m}$ and $r_{n,m}$ are the Doppler shift, phase and envelope of the $n,m$-th component wave respectively and subscript $n,m$ denotes the effect of plane wave $m$ on plane wave $n$. Exploiting the assumed statistical independence of all these random quantities, traditional Rayleigh fading models assume that $I_n(t)$ and $Q_n(t)$ are mutually independent i.i.d. zero mean Gaussian random variables (by virtue of the Central Limit Theorem and exploiting the sum relation in (2.3) and (2.4)). Therefore, by a transformation of random variables, the signal envelope at the receiver, $r(t) = \sqrt{I_n(t)^2 + Q_n(t)^2}$ is Rayleigh distributed. The received signal power, $r(t)^2$ is exponentially distributed, again by a transformation of random variables.

The dynamic generalizations of Rayleigh short-term fading effects are now discussed. Referring back to (2.3) and (2.4), instead of assuming that $I_n(t)$ and $Q_n(t)$ are given by i.i.d. Gaussian random variables, the continuous-time generalizations in [4, 27, 28] model them to be stochastic processes given by the solutions of the following first order linear SDEs

$$dI_n(t) = -\frac{1}{2}\alpha I_n(t)dt + \frac{1}{2}\sigma dW_{I_n}(t), \qquad I_n(0) = (I_n)_0, \qquad t \in \mathbb{R}_+, \tag{2.5}$$

$$dQ_n(t) = -\frac{1}{2}\alpha Q_n(t)dt + \frac{1}{2}\sigma dW_{Q_n}(t), \qquad Q_n(0) = (Q_n)_0, \qquad t \in \mathbb{R}_+, \tag{2.6}$$

where $\alpha > 0$, $\sigma > 0$ and $W_{I_n}(t)$ and $W_{Q_n}(t)$ are independent standard Wiener processes. Here, the processes are randomly drifting around their long-term mean value of zero. In the long term, the processes described by the above SDEs have steady state distributions which are independent Gaussian with zero mean and the same variance.

Applying the transformation $\chi_n(t) = I_n(t)^2 + Q_n(t)^2$ which is the process describing the square envelope or instantaneous power of the received signal, using Ito's rule and using Levy's characterization theorem [4], the following SDE describes the dynamics of the process $\chi_n(t)$

$$d\chi_n(t) = \left(\frac{\sigma^2}{2} - \alpha\chi_n(t)\right) dt + \sigma\sqrt{\chi_n(t)}dW_n(t), \quad t \in \mathbb{R}_+, \tag{2.7}$$

with $\chi_n(0) = I_n(0)^2 + Q_n(0)^2$. The corresponding signal envelope $r(t) = \sqrt{\chi_n(t)}$ is a stochastic process which is Rayleigh distributed as $t$ goes to infinity. Also, if it is initially Rayleigh distributed, it will remain Rayleigh distributed, therefore remaining consistent with the traditional model for Rayleigh short-term fading.

It should be discussed that the $\chi$ process describing the signal output power after short-term fading effects has some guarantees on its positivity in order to assure that the process is well defined for the particular application. In fact, processes described by SDEs of the form

$$dx(t) = a\,(b - x(t))\, dt + \sigma\sqrt{x(t)}dW(t), \quad x(0) = x_0, \quad t \in \mathbb{R}_+, \tag{2.8}$$

are frequently used in financial applications in order to describe interest rates which, in their real world application, must remain positive. This model is called the Cox-Ingersoll-Ross (CIR) model introduced in [30] and is very popular in the literature.

An important result of Feller [31], based on analysis of the associated Fokker-Planck-Kolmogorov (FPK) equation, is that if $2ab \geq \sigma^2$, then this process will remain positive a.s. if its initial condition is positive. For the $\chi$ process described in (2.7), the parameters of the SDE are such that this Feller inequality is met and therefore, the process will indeed remain positive almost surely.

## 2.3 The Concatenated Channel Model

The proposed model aims to model the particular situation in wireless communication systems where the transmitted signal travels reasonably large distances to the local area of the receiver, meanwhile being affected by path loss and long-term fading effects due to reflections off of objects, and then scattering in the local area of the receiver and being reassembled at the receiver, corresponding to local area short-term fading effects. Fig. 2.1 illustrates the scenario being modelled.

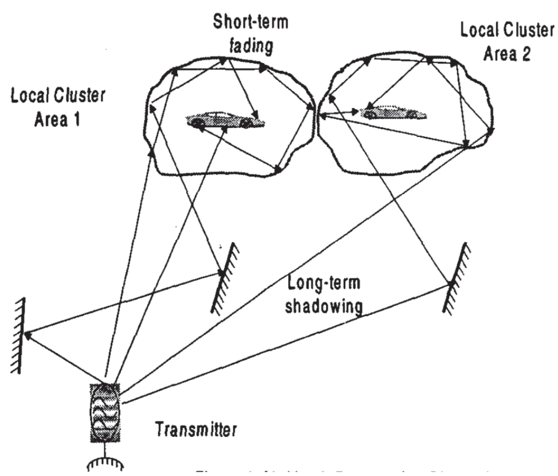


**Fig. 2.1** Concatenated channel model physical scenario taken from [4]

The proposed model further restricts attention to the physical situation where there is no major line of sight (LOS) signal component between transmitter and receiver and therefore short-term fading effects are considered using continuous time Rayleigh fading generalized models as described in Section 2.2. Further, the model does not consider Doppler effects or frequency selective behaviour (it is assumed that the channel is a flat-fading channel).

Evidently the proposed model aims to characterize a concatenation of long-term and short-term fading effects. Each of these effects will be modelled as stochastic processes whose dynamics are governed by a corresponding SDE. The block diagram in Fig. 2.2 compactly depicts the processes governing the short and long-term fading effects which will be developed in this chapter.

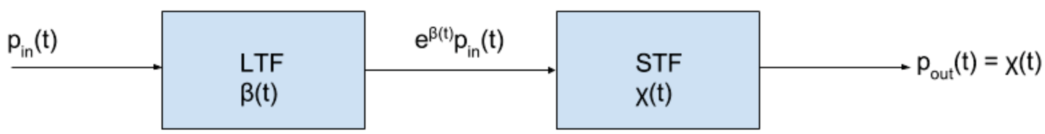


**Fig. 2.2** Channel model block diagram

Here, $p_{in}(t)$ and $p_{out}(t)$ are the channel input and output power respectively, $\beta(t)$ is a long-term fading attenuation process and $\chi(t)$ is the process governing the output power of the short-term fading portion of the channel. The "LTF" and "STF" blocks are understood to be the long-term and short-term fading portions of the channel respectively in the overall concatenated model. The dynamics of the two processes are now defined.

### 2.3.1 The Long-term Fading Process

The long-term fading attenuation process $\beta(t) \in \mathbb{R}$ is modelled by the following the first order linear SDE

$$d\beta(t) = -a(\beta(t) + b)dt + \sigma_\beta dW_\beta(t), \quad \beta(0) = \beta_0, \quad t \in \mathbb{R}_+, \tag{2.9}$$

as in (2.1) where $a > 0$, $b > 0$, $\sigma_\beta > 0$ and $W_\beta(t)$ is a standard Wiener process. The signal power output of the long-term fading portion of the channel is given by $e^{\beta(t)} p_{in}(t)$.

### 2.3.2 The Short-term Fading Process

For the short-term fading process $\chi(t) \in \mathbb{R}_+$, we begin with the SDE model

$$d\chi(t) = \left(\frac{\sigma_\chi^2}{2} - \alpha\chi(t)\right) dt + \sigma_\chi \sqrt{\chi(t)} dW_\chi(t), \quad \chi(0) = \chi_0, \quad t \in \mathbb{R}_+, \tag{2.10}$$

as in (2.7) where $\sigma_\chi > 0$, $\alpha > 0$ and $W_\chi(t)$ is a standard Wiener process. Using this SDE model, the long-term average signal power of the short-term fading channel may be verified to be given by $\frac{\sigma_\chi^2}{2\alpha}$ as stated in [4] and as shown in Appendix C. In the proposed model, this long-term average signal power corresponds exactly to the output signal power (now time varying) of the long-term fading portion of the channel. Explicitly, we substitute $\frac{\sigma_\chi^2}{2\alpha} = e^{\beta(t)} p_{in}(t)$ into (2.10) with the resulting SDE (after substitution) given by (2.11) below.

$$d\chi(t) = \frac{\sigma_\chi^2}{2}\left(1 - \frac{\chi(t)}{e^{\beta(t)} p_{in}(t)}\right) dt + \sigma_\chi \sqrt{\chi(t)} dW_\chi(t), \quad \chi(0) = \chi_0, \quad t \in \mathbb{R}_+, \tag{2.11}$$

Until this point, the dynamical processes being modelled closely follow the techniques described in Section 2.2 for the modelling of short-term fading and long-term fading effects in isolation and uses a coupling of two equations of the form of (2.1) and (2.7) which are linked by the long term average signal envelope (given by $\frac{\sigma_\chi^2}{2\alpha}$ in (2.10)). In the case of this new model, and in contrast to the individual models described in Section 2.2, the long term average signal envelope, $\frac{\sigma_\chi^2}{2\alpha} = e^{\beta(t)} p_{in}(t)$, is time varying and corresponds to the output power of the long-term fading portion of channel. This follows the traditional modelling principle which states that over sufficient lengths of time, long-term fading effects are the average of short-term fading effects [1].

A small parameter $\nu$, where $0 < \nu << 1$, is now introduced in order to remove the singularity when $p_{in}(t) = 0$ resulting in (2.12) below.

$$d\chi(t) = \frac{\sigma_\chi^2}{2}\left(1 - \frac{\chi(t)}{e^{\beta(t)}p_{in}(t) + \nu}\right)dt + \sigma_\chi\sqrt{\chi(t)}dW_\chi(t), \quad \chi(0) = \chi_0, \quad t \in \mathbb{R}_+, \tag{2.12}$$

This parameter is introduced for both analysis purposes and also to take account for the behaviour of the short-term fading portion of the channel when the input power (of that portion of the channel), $e^{\beta(t)}p_{in}(t)$, is equal to zero by assuming that there is always thermal noise present in the long-term fading effects of the channel.

### 2.3.3 Slow-fast Dynamics

Following the work described in [32, 33, 34] multiple time scale dynamics are now applied by using a time scale separation of the two fading processes. We apply the crucial modelling assumption that the long-term fading and short-term fading processes behave in slow time and fast time respectively where "slow time" and "fast time" correspond to the separated time scales after the introduction of a slow-fast parameter $\epsilon$ which is to be defined. The input power of the channel is assumed to be evolving in slow time, in contrast to with the quickly evolving (due to short-term fading effects) output power.

We now provide the relevant equations and then justify the time scale separation from both a modelling and analysis perspective. A small parameter $\epsilon$, $0 < \epsilon << 1$ is introduced into the SDEs in order to separate the slow and fast time components. This is a standard move in modelling deterministic systems with separated time scales but in the SDE case there is the added feature that the diffusion term is scaled by $\frac{1}{\sqrt{\epsilon}}$. The resulting equations (for $t \in \mathbb{R}_+$) are

$$d\beta(t) = -a(\beta(t) + b)dt + \sigma_\beta dW_\beta(t), \quad \beta(0) = \beta_0, \tag{2.13}$$

$$d\chi(t) = \frac{1}{\epsilon}\frac{(\sigma_\chi)^2}{2}\left(1 - \frac{\chi(t)}{e^{\beta(t)}p_{in}(t) + \nu}\right)dt + \frac{\sigma_\chi}{\sqrt{\epsilon}}\sqrt{\chi(t)}dW_\chi(t), \quad \chi(0) = \chi_0, \tag{2.14}$$

where $\chi(t)$ is the fast time process and $\beta(t)$ is the slow time process.

From the point of view of accurate modelling, the effects of short-term fading occur in the order of milliseconds which is significantly faster than the effects of long-term fading which occur in the order of seconds, as discussed in Chapter 1. In particular, the influence of the long-term fading signal output power $e^{\beta(t)}p_{in}(t)+\nu$ is almost constant with respect to the dynamics of the short-term fading phenomena. The long-term fading signal output power can be thought of as the average to which the complete channel output power (after short-term fading effects) is tracking which is an important desired goal of the proposed model. Therefore, a time scale separation is necessary in order to have an accurate model of the interaction of the two fading processes.

From the perspective of analysis, a key result in slow-fast dynamical systems is that as the slow-fast parameter $\epsilon$ goes to zero, the slow-time process is asymptotically constant in terms of its influence on the fast-time process. This result justifies the ability to use a substitution of the form $\frac{\sigma_\chi^2}{2\alpha} = e^{\beta(t)}p_{in}(t) + \nu$ which corresponds to the substitution of a constant SDE parameter by a random time varying process. The application of a time scale separation into slow and fast time processes is such that the slow-time process $e^{\beta(t)}p_{in}(t)+\nu$, which explicitly appears in the SDE of the fast-time process $\chi(t)$, is constant in terms of its influence on $\chi(t)$ thus eliminating any potential complications in the algebraic substitution of a constant by a time-varying process. Also, the separation of time scales allows for the development of transition densities for the processes which will be described in Section 2.4.

### 2.3.4 The Summarized Model

The complete channel model is now summarized by providing the SDEs for the model which include all relevant modelling assumptions made. The equations (for

$t \in \mathbb{R}_+$) are

$$d\beta(t) = -a(\beta(t) + b)dt + \sigma_\beta dW_\beta(t), \quad \beta(0) = \beta_0, \tag{2.15}$$

$$dp_{out}(t) = \frac{1}{\epsilon}\frac{(\sigma_{p_{out}})^2}{2}\left(1 - \frac{p_{out}(t)}{e^{\beta(t)}p_{in}(t) + \nu}\right)dt + \frac{\sigma_{p_{out}}}{\sqrt{\epsilon}}\sqrt{p_{out}(t)}dW_{p_{out}}(t), \tag{2.16}$$

$$p_{out}(0) = (p_{out})_0,$$

noting the substitution of $\chi(t) = p_{out}(t)$ and also noting the relabelling of the $\sigma_{p_{out}}$ and $W_{p_{out}}$ terms for consistency of notation thus completing the mathematical model.

## 2.4 Transition Densities

The transition densities for the processes governing the channel dynamics are now presented.

### 2.4.1 The Long-term Fading Process

We begin with the transition density for the long-term fading channel gain $S(t) = e^{\beta(t)}$. From [4], the transition density for the value $S_t$ of $S(t)$ at time $t \in \mathbb{R}_+$, conditional on the value $S_s$ at time $s \in \mathbb{R}_+,\ \ s < t$ and the parameter set $\theta$ of the SDE (2.15), is given below.

$$f_\theta(S_t, t; S_s, s) = \frac{1}{\sqrt{2\pi(t-s)\sigma_\beta^2}S_t} e^{\left(-\frac{\left(\log\frac{S_t}{S_s} + b(t-s)\right)^2}{2(t-s)\sigma_\beta^2}\right)} \tag{2.17}$$

Following [4], letting $t \to \infty$, the asymptotic transition density is given by

$$f_\theta(S_\infty, \infty; S_s, s) = \frac{1}{\sqrt{2\pi\frac{\sigma_\beta^2}{2a}}S_\infty} e^{\left(-\frac{\left(\log\frac{S_\infty}{S_s} + b\right)^2}{2\left(\frac{\sigma_\beta^2}{2a}\right)}\right)} \tag{2.18}$$

for $S_\infty > 0$, $s \in \mathbb{R}_+$, which is the density of a log-normal random variable with mean $e^{b-logS_s+\frac{\sigma_\beta^2}{4a}}$ and variance $(e^{\frac{\sigma_\beta^2}{2a}}-1)e^{2(b-logS_s)+\frac{\sigma_\beta^2}{4a}}$ and where the associated normal random variable has mean $b-logS_s$ and variance $\frac{\sigma_\beta^2}{2a}$. Therefore, as $t$ goes to infinity, $S(t)$ is log-normally distributed given its current value $S_s$ at time $s$ and the SDE parameters. Therefore, at the macroscopic level, the modelling of the long-term fading effects reduces to the traditional log-normal model, as is argued in [4].

### 2.4.2 The Short-term Fading Process

Similar to the long-term fading process, we present the transition density for the $\chi(t)$ process which represents the output power of the channel after short-term fading effects. A key consequence of the time separation of slow-fast dynamics of the system model (2.15) - (2.16) is that from the perspective of the fast-time equation (that of the $\chi(t)$ process), the slow time processes $\beta(t)$ and $p_{in}(t)$ appear almost constant. Therefore, following from [4], the transition density for the value $\chi_t$ of $\chi(t)$ at time $t \in \mathbb{R}_+$, conditional on the value $\chi_s$ at time $s \in \mathbb{R}_+$, $s < t$, the values of $\beta_s$ and $(p_{in})_s$ (which due to the slow-fast dynamical relationship are assumed to remain almost constant) at time $s$ and the parameter set $\theta$ of the SDE (2.16), is given by

$$f_\theta(\chi_t, t; \chi_s, \beta_s, (p_{in})_s, s) = \frac{1}{2\mu} e^{\left(-\frac{\lambda+\chi_t}{2\mu}\right)} I_0\left(\frac{\sqrt{\chi_t\lambda}}{\mu}\right) \tag{2.19}$$

where

$$\mu = \frac{e^{\beta_s}(p_{in})_s + \nu}{2}\left(1 - e^{\left(-\frac{\sigma_{p_{out}}^2}{2\epsilon}\frac{1}{e^{\beta_s}(p_{in})_s+\nu}(t-s)\right)}\right) \tag{2.20}$$

$$\lambda = \chi_s e^{\left(-\frac{\sigma_{p_{out}}^2}{2\epsilon}\frac{1}{e^{\beta_s}(p_{in})_s+\nu}(t-s)\right)} \tag{2.21}$$

and $I_0(\cdot)$ is the modified Bessel function of the first kind of zero-th order. Following from [4], letting $t \to \infty$, the asymptotic transition density is given by

$$f_\theta(\chi_\infty, \infty; \chi_s, \beta_s, (p_{in})_s, s) = \frac{1}{e^{\beta_s}(p_{in})_s + \nu} e^{-\left(\frac{1}{e^{\beta_s}(p_{in})_s+\nu}\chi_\infty\right)} \tag{2.22}$$

for $\chi_\infty > 0$, $s \in \mathbb{R}_+$, which is the density of an exponential random variable with mean $e^{\beta_s}(p_{in})_s + \nu$. Therefore, as $t$ goes to infinity, $p_{out}(t) = \chi(t)$ is exponentially distributed given its current value $\chi_s$ at time $s$, the values of $\beta_s$ and $(p_{in})_s$ at time $s$, and the SDE parameters. In other words, given the current value of the signal power $e^{\beta_s}(p_{in})_s + \nu$ after long-term fading effects have occured at time $s$, the current output power of the channel $\chi_s$ at time $s$, and all SDE parameters, the output power of the short-term fading portion of the channel $\chi_t$ at time $t$ is exponentially distributed as $t$ goes to infinity.

A simple transformation of random variables $r = \sqrt{\chi}$ describes the square root of the output power of the channel and is effectively the signal magnitude (envelope). Then the asymptotic transition density for $r$ is a Rayleigh density by the known fact that the square root of an exponential random variable is a Rayleigh random variable. Therefore, at the macroscopic level, the modelling of the short-term fading effects reduce to the traditional Rayleigh fading model, as is argued in [4].

The asymptotic transition densities of both fading processes in the new channel model show that the model reduces to the traditional models described in the literature over long periods of time. The model also introduces continuous time dynamics which in small time scales introduce a new dimension to the statistical channel information.

## 2.5 Channel Simulations

Simulations are now presented in order to verify the channel model. In particular, simulations are first shown for the sample path behaviour of the channel under different parameters and inputs. Then, a large number of sample paths of the channel are computed in order to verify the empirical distribution of channel process states after long periods of time have elapsed and the empirical histograms of these samples are compared to the asymptotic transition densities described in Section 2.4.

### 2.5.1 Sample Path Simulations

Two sample paths of the proposed SDE channel model are now illustrated using simulation. As presented in Section 2.3.4, the simulated SDEs of interest describing the dynamics of the channel model are given in (2.23) and (2.24) below

$$d\beta(t) = -a(\beta(t) + b)dt + \sigma_\beta dW_\beta(t), \quad \beta(0) = \beta_0, \tag{2.23}$$

$$dp_{out}(t) = \frac{1}{\epsilon}\frac{(\sigma_{p_{out}})^2}{2}\left(1 - \frac{p_{out}(t)}{e^{\beta(t)}p_{in}(t) + \nu}\right)dt + \frac{\sigma_{p_{out}}}{\sqrt{\epsilon}}\sqrt{p_{out}(t)}dW_{p_{out}}(t),$$
$$p_{out}(0) = (p_{out})_0, \tag{2.24}$$

where $t \in \mathbb{R}_+$.

#### Constant Transmit Power

First, the channel is simulated using a constant transmit power $p_{in}(t) = 1$ for all $t$. The SDE parameters are set to be $\epsilon = 0.01$, $\nu = 0$, $a = 10$, $b = 0$, $\sigma_\beta = 0.2$, $\sigma_{p_{out}} = 0.8$. The process initial conditions are set to be $\beta_0 = 0$ and $(p_{out})_0 = 1$. Fig. 2.3 shows the result of the simulation.

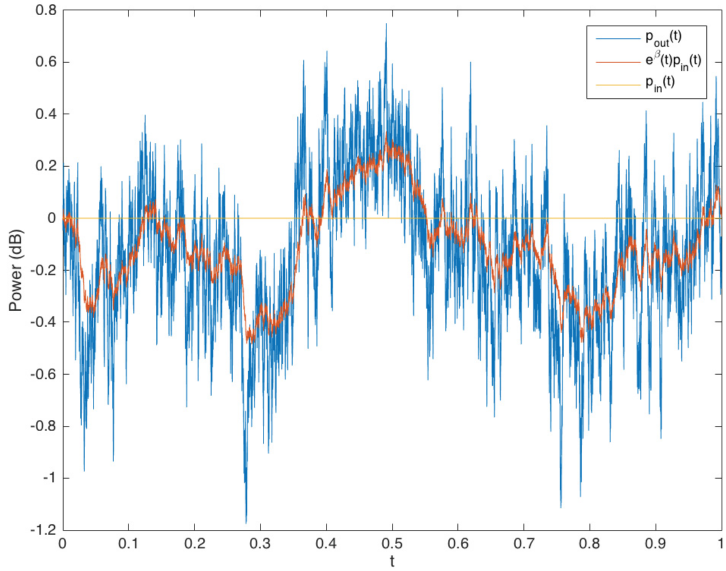


**Fig. 2.3** Example channel sample path: constant transmit power

From the plot one can see that the long-term fading output signal power, $e^{\beta(t)}p_{in}(t)$, is oscillating (with stochastic disturbances) around the average long-term fading output power $e^{-b}p_{in}(t) = e^0 \cdot 1 = 1$ and is acting as an average to which the short-term fading output power $p_{out}(t)$ is tracking. One also can see that the volatility of the short-term fading effects is more drastic and is occurring at a much faster time scale.

### Sinusoidal Transmit Power

Time varying transmit power is now introduced in the form of the sinusoid $p_{in}(t) = 0.5\sin(t) + 1$ for all $t$. The SDE parameters are set to be $\epsilon = 0.01$, $\nu = 0$, $a = 10$, $b = 0$, $\sigma_\beta = 0.2$, $\sigma_{p_{out}} = 2$. The process initial conditions are set as $\beta_0 = 0$ and $(p_{out})_0 = 1$. Fig. 2.4 shows the results of the simulation.

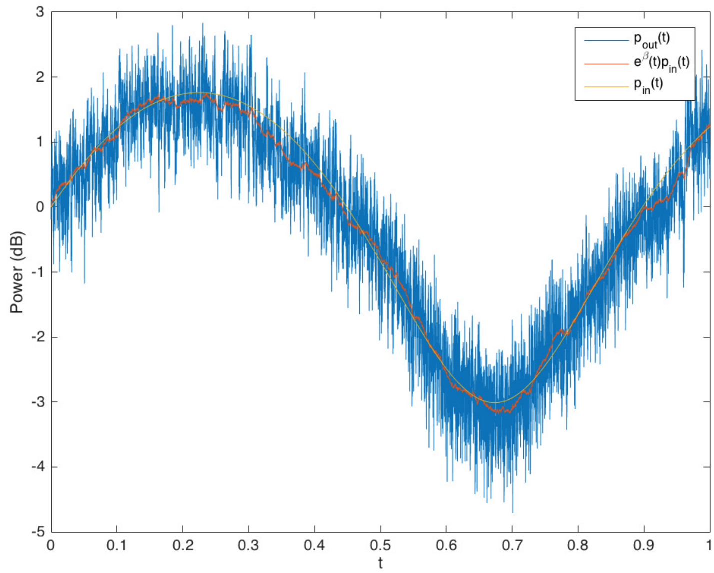


**Fig. 2.4** Example channel sample path: sinusoidal transmit power

Here the long-term fading output power $e^{\beta(t)}p_{in}(t)$ is slowly tracking the input sinusoid while the short-term fading output power $p_{out}(t)$ is rapidly and randomly oscillating about $e^{\beta(t)}p_{in}(t)$ as expected.

### 2.5.2 Empirical Verification of Transition Densities

Simulations are also developed in order to verify that the empirical distributions of process values are consistent with the asymptotic transition densities described in Section 2.4 given a large number of samples and a long enough period of time. Considering the channel SDEs

$$d\beta(t) = -a(\beta(t) + b)dt + \sigma_\beta dW_\beta(t), \quad \beta(0) = \beta_0, \tag{2.25}$$

$$dp_{out}(t) = \frac{1}{\epsilon}\frac{(\sigma_{p_{out}})^2}{2}\left(1 - \frac{p_{out}(t)}{e^{\beta(t)}p_{in}(t) + \nu}\right)dt + \frac{\sigma_{p_{out}}}{\sqrt{\epsilon}}\sqrt{p_{out}(t)}dW_{p_{out}}(t),$$
$$p_{out}(0) = (p_{out})_0, \tag{2.26}$$

$t \in \mathbb{R}_+$, the parameters are set to be $b = 0$, $a = 10$, $\sigma_\beta = 1$, $\sigma_{p_{out}} = 0.8$, $\epsilon = 0.01$ and $\nu = 0$. We now simulate $N = 1000$ sample paths of the channel processes denoted $(\beta^i(t), p^i_{out}(t))$, $1 \leq i \leq N$ until final time $T > 0$ with constant transmit power $p^i_{in}(t) = 1$ for all $t \in [0, T]$ and the initial conditions $\beta^i(0) = 0$, $p^i_{out}(0) = 1$ for all $i$. The $N$ sample paths of the channel are simulated until terminal time $T = 1$ which corresponds in the case of this simulation to be approximately infinite. We then compute the normalized (to an area of 1) empirical histogram of the values of $e^{\beta^i(T)}$ and $p^i_{out}(T)$ corresponding to the long-term fading power gain and short-term fading output power of the channel respectively at $T = 1$. This empirical data is compared with the expected asymptotic transition densities for the long-term fading gain and short-term fading output power given by (2.18) and (2.22) respectively, substituting all SDE parameters and initial conditions. Fig. 2.5 and 2.6 show the results of the simulations.

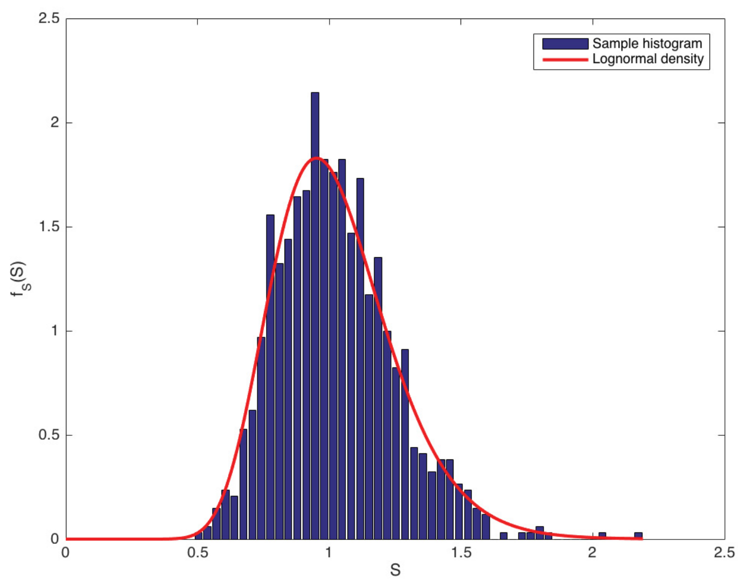


**Fig. 2.5** Asymptotic transition density (2.18) versus sample histogram of long-term fading attenuation coefficient $S(T)$

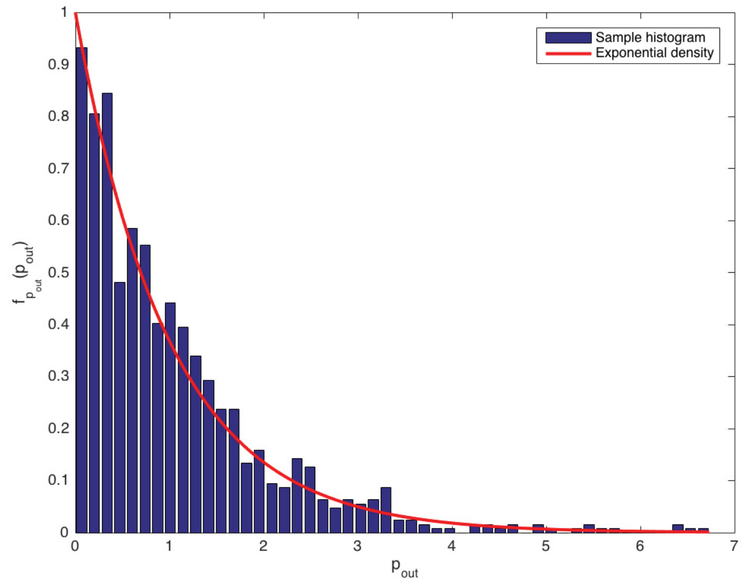


**Fig. 2.6** Asymptotic transition density (2.22) versus sample histogram of channel output power $p_{out}(T)$

Both simulations show that the state values of a large number of paths over a long period of time are distributed close to the asymptotic transition densities described in Section 2.4 (in terms of sample histograms) confirming these densities numerically and also re-iterating that the model reduces to the traditional log-normal and Rayleigh fading models at the high level.

## 2.6 Extended Models Using Poisson Jumps

### 2.6.1 The Channel Model Extension

An extension to the proposed model developed in Section 2.3 is now presented. This extended model aims to describe a special scenario in the proposed base model where the long-term fading effects include a significant drop or increase in gain due to the presence of large obstacles. This new modelling challenge is addressed by introducing jump processes to the proposed model. In particular, we begin with the base model described in (2.15) and (2.16) and introduce a jump term $dJ^{\lambda}(t)$ into the

SDE describing the dynamics of the long-term fading variable $\beta(t)$. The resulting system equations (for $t \in \mathbb{R}_+$) are given below.

$$d\beta(t) = -a(\beta(t) + b)dt + \sigma_\beta dW_\beta(t) + dJ^\lambda(t), \quad \beta(0) = \beta_0, \tag{2.27}$$

$$dp_{out}(t) = \frac{1}{\epsilon}\frac{(\sigma_{p_{out}})^2}{2}\left(1 - \frac{p_{out}(t)}{e^{\beta(t)}p_{in}(t) + \nu}\right)dt + \frac{\sigma_{p_{out}}}{\sqrt{\epsilon}}\sqrt{p_{out}(t)}dW_{p_{out}}(t), \quad p_{out}(0) = (p_{out})_0 \tag{2.28}$$

Here, all variables and parameters are defined as before and the new addition $J^\lambda(t)$ is a Poisson process with parameter $\lambda$, independent of all other random phenomena (including the Brownian motion). The Poisson rate $\lambda$ is taken to model the average number of large obstacles encountered by a moving device over a normalized time period of 1. The Poisson process takes jumps of height 1 and $-1$ with equal probability 1/2. The Poisson process effectively models the rapid jumps in long-term fading channel gain due to a moving transmitting device being immediately blocked by a large obstacle (corresponding to a negative jump) or immediately leaving the obstacles shadowing area (corresponding to a positive jump).

### 2.6.2 Sample Path Simulation

A sample path of the extended model (2.27), (2.28) is now simulated in order to verify the behaviour of the channel in the presence of jumps. Setting the Poisson parameter $\lambda$ to 5, the SDE parameters are chosen to be $a = 1$, $b = 0$, $\sigma_\beta = 1$, $\sigma_{p_{out}} = 4$, $\epsilon = 0.01$ and $\nu = 0$. The input power is set to be a constant value $p_{in}(t) = 1$ for all $t$. The initial conditions used are $\beta_0 = 0$, $(p_{out})_0 = 1$. Fig. 2.7 depicts a sample path of the simulated processes.

As shown in the figure, the long-term fading output power is being affected by randomly occurring jumps. Furthermore, the simulations show that the short-term fading output power is still rapidly oscillating around the long-term fading output power even in the presence of these jumps.

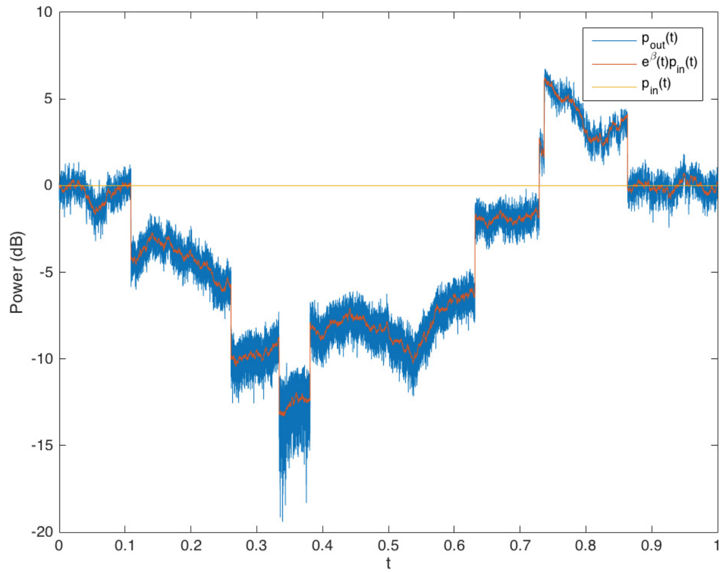


**Fig. 2.7** Example channel sample path with Poisson jumps and constant transmit power

# Chapter 3

# Decentralized Stochastic Control of CDMA Networks

## 3.1 Introduction

We now consider a decentralized CDMA cellular uplink power control problem where users are transmitting data to a common base station. The system is modelled as a large population competitive game with $N$ different agents or decision makers corresponding to the devices transmitting. The system evolves in continuous time and has finite horizon $0 < T < \infty$. Through the control of their transmit power and motion, agents are competing with each other in order to optimize their own running cost specified by a linear combination of their quality of service (QoS) and transmit power and denoted $c_i$ in (3.1)

$$c_i = -\gamma_i + p_i = -\frac{h_i p_i}{\frac{1}{N}\sum_{j=1, j\neq i}^{n} h_j p_j + \eta} + p_i \tag{3.1}$$

omitting time indices for brevity where $\gamma_i$, $h_i$ and $p_i$ are the signal-to-interference-plus-noise-ratio (SINR), channel gain and transmit power of agent $i$ respectively.

The problem is considered in two forms. First, a game is presented where agent positions in space are abstracted and we only consider agent states involving transmit powers and information of channel attenuation dynamics. Second, we introduce two new state variables corresponding to the agents' two-dimensional position in space and introduce the effects of agent positions in their cost or performance function couplings.

In the case of both problems, namely with and without agent motion and state variables of position, this chapter is organized as follows. First, all state variables, dynamics, and agent cost functions are defined. Then, the system is considered in its infinite population limit resulting in a nonlinear loop of MFG equations of the generic agent. These equations are presented and an existence and uniqueness analysis is conducted on the solutions of these equations as well as the solution of the nonlinear MFG Loop. The work in this chapter closely follows and builds upon the methodology found in [17, 18], with the notable addition of the novel channel model developed in detail in Chapter 2.

In this work, the term optimal is to be understood in the sense of Nash Equilibrium strategies, namely the optimal control of an agent is the best response control to the other agents' controls in the Nash Equilibrium control set and the optimal performance of an agent is the expected performance of the agent when applying the Nash Equilibrium control strategies.

## 3.2 Agent State Variables

At any instant $t \in \mathbb{R}_+$, the *state* of agent $i$, where $1 \leq i \leq N$, consists of three main state variables:

> $\beta^i(t) \in \mathbb{R}$ : the long-term fading parameter of the channel from the agent device to the base station,
>
> $p^i_{in}(t) \in \mathbb{R}^+$ : the transmitted signal power of the agent device,
>
> $p^i_{out}(t) \in \mathbb{R}^+$ : the received signal power at the base station.

In the case agent motion is considered, the following state variables are added:

$$x^i(t) = \begin{pmatrix} x_1^i(t) \\ x_2^i(t) \end{pmatrix} \in \mathbb{R}^2 : \text{ the agent's position in two-dimensional space.}$$

The state variables $\beta^i(t)$, $p_{in}^i(t)$ and $p_{out}^i(t)$ are linked via the nonlinear channel model developed in Chapter 2 which is applied in the work of this chapter and which will be evident in the description of state dynamics in Section 3.3.

## 3.3 State Dynamics and Stochastic Differential Equations

### 3.3.1 Rate Based Power Control

Gradient type methods are common in power control algorithms in the cellphone domain where the transmit power is being adjusted by explicitly updating its rate of change in the form of power up or power down type adjustments [35, 36, 37]. Following the approach in [17, 18], a rate adjustment model of the following form is used:

$$dp_{in}^i(t) = u_{p_{in}}^i(t)dt + \sigma_{p_{in}}^i dW_{p_{in}}^i(t), \quad p_{in}^i(0) = (p_{in}^i)_0, \tag{3.2}$$

where $|u_{p_{in}}^i(t)| \leq u_{p_{max}} = 1$, $\sigma_{p_{in}}^i > 0$, for all $i$ and $W_{p_{in}}^i(t), 1 \leq i \leq N$, are $N$ independent standard Wiener processes and $(p_{in}^i)_0$ is the known initial transmit power. Here, $u_{p_{in}}^i(t)$ corresponds to the power control signal of agent $i$ at the instant $t$.

### 3.3.2 Dynamic Channel State Processes

The channel model used in this work is the basic channel model developed in Chapter 2 which consists of long-term fading from the agent device to the local area of the base station influenced by the state process $\beta^i(t)$, followed by short-term fading in the local area of the base station resulting in the output power state process $p_{out}^i(t)$. Each agent therefore has one state variable for each of these two processes. The dynamics are now described in detail as follows.

**Long-term Fading Process**

Following the model described in Chapter 2, the long-term fading attenuation process $\beta^i(t)$ for each agent $i$ evolves according to the following SDE

$$d\beta^i(t) = -a^i(\beta^i(t) + b^i)dt + \sigma^i_\beta dW^i_\beta(t), \quad \beta^i(0) = \beta^i_0, \tag{3.3}$$

where $a^i > 0, b^i > 0$ and $\sigma^i_\beta > 0$, for all $i$. Also, $W^i_\beta(t), 1 \le i \le N$ are $N$ independent standard Wiener processes and $\beta^i_0$, $1 \le i \le N$ are mutually independent Gaussian random variables which is are also independent of the Wiener processes.

**Received Signal Power at the Base Station**

Again following the model in Chapter 2, for each agent $i$, the signal received power, $p^i_{out}(t)$, is governed by the following SDE:

$$dp^i_{out}(t) = \frac{(\sigma^i_{p_{out}})^2}{2}\left(1 - \frac{p^i_{out}(t)}{e^{\beta^i(t)}p^i_{in}(t) + \nu}\right)dt + \sigma^i_{p_{out}}\sqrt{p^i_{out}(t)}dW^i_{p_{out}}(t),$$

$$p^i_{out}(0) = (p^i_{out})_0, \tag{3.4}$$

where $\sigma^i_{p_{out}} > 0$, for all $i$. Also, $W^i_{p_{out}}(t), 1 \le i \le N$ are $N$ independent standard Wiener processes.

### 3.3.3 Agent Position in Space

Agent motion is modelled as stepwise adjustments using the rate adjustment model as in [17, 18]; these stepwise adjustments are then described by the following SDEs

$$dx^i_1(t) = u^i_{x_1}(t)dt + \sigma^i_{x_1}dW^i_{x_1}(t), \quad x^i_1(0) = (x^i_1)_0 \tag{3.5}$$

$$dx^i_2(t) = u^i_{x_2}(t)dt + \sigma^i_{x_2}dW^i_{x_2}(t), \quad x^i_2(0) = (x^i_2)_0 \tag{3.6}$$

where $|u^i_{x_1}(t)|, |u^i_{x_2}(t)| \leq u_{x_{max}} = 1$ are the position controls of agent $i$, $\sigma^i_{x_1} > 0$, $\sigma^i_{x_2} > 0$ for all $i$. Also, $W^i_{x_1}(t), 1 \leq i \leq N$ are $N$ independent standard Wiener processes independent of mutually independent $W^i_{x_2}(t), 1 \leq i \leq N$ and $(x^i_1)_0$ and $(x^i_2)_0$ is the known initial position.

## 3.4 Slow-fast Dynamics

Capturing the above state variables into one complete model for each of the two situations of interest (with and without agent motion), we must first distinguish the fast and slow components of the agent state where the terms "slow time" and "fast time" correspond to the separated time scales after the introduction of a slow-fast parameter $\epsilon$ which is to be defined.

As justified in Chapter 2, $\beta^i(t)$ and $p^i_{out}(t)$ are categorized into slow and fast variables respectively. It is further assumed that the power updates occur in slow time, i.e. the SDE governing the state variable $p^i_{in}(t)$ evolves at the same rate as $\beta^i(t)$ which is orders of magnitude slower than the dynamics of the channel output power $p^i_{out}(t)$. In the case of the work with agent positions and motion, agents are assumed to be moving in slow time.

To model the separation of fast and slow components of the state a small parameter $0 < \epsilon << 1$ is introduced. As remarked in Chapter 2, this is a standard move in modelling deterministic systems with separated time scales, but in the SDE case there is the added feature that the diffusion term is scaled by $\frac{1}{\sqrt{\epsilon}}$. The modified main state variable SDEs of agent $i$ are given below.

$$d\beta^i(t) = -a^i(\beta^i(t) + b^i)dt + \sigma^i_\beta dW^i_\beta(t), \quad \beta^i(0) = \beta^i_0 \tag{3.7}$$

$$dp^i_{in}(t) = u^i_{p_{in}}(t)dt + \sigma^i_{p_{in}} dW^i_{p_{in}}(t), \quad p^i_{in}(0) = (p^i_{in})_0 \tag{3.8}$$

$$dp^i_{out}(t) = \frac{1}{\epsilon}\frac{(\sigma^i_{p_{out}})^2}{2}\left(1 - \frac{p^i_{out}(t)}{e^{\beta^i(t)}p^i_{in}(t) + \nu}\right)dt + \frac{1}{\sqrt{\epsilon}}\sigma^i_{p_{out}}\sqrt{p^i_{out}(t)}dW^i_{p_{out}}(t), \tag{3.9}$$

$$p^i_{out}(0) = (p^i_{out})_0,$$

If agent motion is included in the model, the following equations are added.

$$dx_1^i(t) = u_{x_1}^i(t)dt + \sigma_{x_1}^i dW_{x_1}^i(t), \quad x_1^i(0) = (x_1^i)_0 \tag{3.10}$$

$$dx_2^i(t) = u_{x_2}^i(t)dt + \sigma_{x_2}^i dW_{x_2}^i(t), \quad x_2^i(0) = (x_2^i)_0 \tag{3.11}$$

## 3.5 Uniform Dynamics and Combined State Variables

We now develop complete models including both agent channel and transmit power and space configuration states. This work considers only the case of uniform agents, namely the case where all agents have identical SDE parameters governing their state dynamics. All indices $i$ associated to SDE parameters in the dynamical equations are therefore dropped.

### 3.5.1 Models Without Localized Cost or Agent Motion

In the case where agent motion is not included, an agent $i$'s state can be given by the state vector $\theta^i(t) = \begin{pmatrix} \beta^i(t) & p_{in}^i(t) & p_{out}^i(t) \end{pmatrix}^T$ with corresponding SDE dynamics

$$d\theta^i(t) = \begin{pmatrix} -a(\beta^i(t) + b) \\ u_{p_{in}}^i(t) \\ \frac{1}{\epsilon}\frac{(\sigma_{p_{out}})^2}{2}\left(1 - \frac{p_{out}^i(t)}{e^{\beta^i(t)}p_{in}^i(t)+\nu}\right) \end{pmatrix} dt + \begin{pmatrix} \sigma_\beta & 0 & 0 \\ 0 & \sigma_{p_{in}} & 0 \\ 0 & 0 & \frac{1}{\sqrt{\epsilon}}\sigma_{p_{out}}\sqrt{p_{out}^i(t)} \end{pmatrix} dW^i(t) \tag{3.12}$$

where all parameters are defined as before and $W^i(t) = \begin{pmatrix} W_\beta^i(t) & W_{p_{in}}^i(t) & W_{p_{out}}^i(t) \end{pmatrix}^T$ are mutually independent Wiener processes and $\theta^i(0) = \begin{pmatrix} \beta^i(0) & p_{in}^i(0) & p_{out}^i(0) \end{pmatrix}^T$ is the initial state value.

### 3.5.2 Models With Localized Cost and Agent Motion

In the case where agent motion is included, an agent $i$'s state can be given by the state vector $\theta^i(t) = \begin{pmatrix} \beta^i(t) & p_{in}^i(t) & p_{out}^i(t) & x_1^i(t) & x_2^i(t) \end{pmatrix}^T$ with corresponding SDE dynamics

$$
d\theta^i(t) = \begin{pmatrix} -a(\beta^i(t)+b) \\ u^i_{p_{in}}(t) \\ \frac{1}{\epsilon}\frac{(\sigma_{p_{out}})^2}{2}\left(1 - \frac{p^i_{out}(t)}{e^{\beta^i(t)}p^i_{in}(t)+\nu}\right) \\ u^i_{x_1}(t) \\ u^i_{x_2}(t) \end{pmatrix} dt \quad + \begin{pmatrix} \sigma_\beta & 0 & 0 & 0 & 0 \\ 0 & \sigma_{p_{in}} & 0 & 0 & 0 \\ 0 & 0 & \frac{1}{\sqrt{\epsilon}}\sigma_{p_{out}}\sqrt{p^i_{out}(t)} & 0 & 0 \\ 0 & 0 & 0 & \sigma_{x_1} & 0 \\ 0 & 0 & 0 & 0 & \sigma_{x_2} \end{pmatrix} dW^i(t) \tag{3.13}
$$

where $W^i(t) = \begin{pmatrix} W^i_\beta(t) & W^i_{p_{in}}(t) & W^i_{p_{out}}(t) & W^i_{x_1}(t) & W^i_{x_2}(t) \end{pmatrix}^T$ are mutually independent Wiener processes and $\theta^i(0) = \begin{pmatrix} \beta^i(0) & p^i_{in}(0) & p^i_{out}(0) & x^i_1(0) & x^i_2(0) \end{pmatrix}^T$ is the initial state value.

## 3.6 Agent Cost Functions

### 3.6.1 Models Without Localized Cost or Agent Motion

In order to quantify an agent's cost, two important metrics are used: QoS and power consumption. Here, QoS will be defined as the SINR of the transmitted signal over the wireless channel. The SINR of agent $i$, $1 \le i \le N$ is given by the expression

$$
\gamma_i(t) \triangleq \frac{p^i_{out}(t)}{\frac{1}{N}\sum_{k=1,k\neq i}^{N} p^k_{out}(t) + \eta} \tag{3.14}
$$

where $\eta$ is the channel noise power. We then define

$$\kappa_i(t) \triangleq \frac{p^i_{out}(t)}{\frac{1}{N}\sum_{k=1}^N p^k_{out}(t) + \eta} \tag{3.15}$$

Here $\kappa_i(t)$ and $\gamma_i(t)$ differ by the $k \neq i$ sum restriction in the formulation of $\gamma_i(t)$ but it is proven in Lemma 1 of [17] that subject to the condition that $p^i_{out}(u_i)$ is twice continuously differentiable in $u_i$ and $\gamma_i(u_i)$ has a unique minimum in $U = [-1, 1]$ then the unique minimizer of $\gamma_i(t)$ will be equal to the unique minimizer of $\kappa_i(t)$ as they are defined here. Hence, in order to simplify analysis for optimization in the remainder of this work, the QoS $Q_i$ of agent $i$, $1 \leq i \leq N$, shall be defined as follows:

$$Q_i(t) \triangleq \kappa_i(t) = \frac{p^i_{out}(t)}{\frac{1}{N}\sum_{k=1}^N p^k_{out}(t) + \eta}, \qquad t \in \mathbb{R}_+ \tag{3.16}$$

The instantaneous loss of a given agent $i$ in the $N$ agent game is then defined as

$$\begin{aligned} L_i^N(t, u_i, u_{-i}) &\triangleq -Q_i(t) + p^i_{in}(t) && (3.17)\\ &= -\frac{p^i_{out}(t)}{\frac{1}{N}\sum_{k=1}^N p^k_{out}(t) + \eta} + p^i_{in}(t) && (3.18)\end{aligned}$$

The cost-to-go function of agent $i$ is then defined as

$$\begin{aligned} J_i^N(s, u_i, u_{-i}, \tilde{\theta}_i) &\triangleq E\left[\int_s^T L_i^N(t, u_i, u_{-i})dt \middle| \theta_i(s) = \tilde{\theta}_i\right] && (3.19)\\ &= E\left[\int_s^T \left(-\frac{p^i_{out}(t)}{\frac{1}{N}\sum_{k=1}^N p^k_{out}(t) + \eta} + p^i_{in}(t)\right) dt \middle| \theta_i(s) = \tilde{\theta}_i\right] && (3.20)\end{aligned}$$

where $s > 0$ is the current time, $T < \infty$ is the terminal time, $u_i$ denotes the control of agent $i$, $u_{-i}$ denotes the controls of all other agents excluding agent $i$ and $\tilde{\theta}_i$ is the value of $\theta_i(s)$.

### 3.6.2 Models With Localized Cost and Agent Motion

Considering the problem with localized cost and agent motion, a combination of QoS and transmit power is also used in order to define cost functions but in this case, the agent's location in space introduces a new influence on its cost. Deterministic path loss is introduced into the SINR equation as follows

$$Q_i(t) \triangleq \frac{e^{-||x^i(t)-x^b||^2} p^i_{out}(t)}{\frac{1}{N}\sum_{k=1}^{N} e^{-||x^k(t)-x^b||^2} p^k_{out}(t) + \eta} \tag{3.21}$$

where $||\cdot||$ denotes the euclidean norm, $x^i(t) = \begin{pmatrix} x^i_1(t) \\ x^i_2(t) \end{pmatrix}$, and $x^b$ denotes the position of the base station and recalling that path loss corresponds to an exponential drop in received power with respect to the distance travelled by the signal. The instantaneous loss of a given agent $i$ in the $N$ agent game is then defined as

$$L^N_i(t, u_i, u_{-i}) \triangleq -Q_i(t) + p^i_{in}(t) \tag{3.22}$$

$$= -\frac{e^{-||x^i(t)-x^b||^2} p^i_{out}(t)}{\frac{1}{N}\sum_{k=1}^{N} e^{-||x^k(t)-x^b||^2} p^k_{out}(t) + \eta} + p^i_{in}(t) \tag{3.23}$$

The cost-to-go function of agent $i$ is then defined as

$$J^N_i(s, u_i, u_{-i}, \tilde{\theta}_i) \triangleq E\left[\int_s^T L^N_i(t, u_i, u_{-i})dt \middle| \theta_i(s) = \tilde{\theta}_i\right] \tag{3.24}$$

$$= E\left[\int_s^T \left(-\frac{e^{-||x^i(t)-x^b||^2} p^i_{out}(t)}{\frac{1}{N}\sum_{k=1}^{N} e^{-||x^k(t)-x^b||^2} p^k_{out}(t) + \eta} + p^i_{in}(t)\right) dt \middle| \theta_i(s) = \tilde{\theta}_i\right] \tag{3.25}$$

where $s > 0$ is the current time and $T < \infty$ is the terminal time.

## 3.7 Mean Field Games Analysis

A MFG analysis is now applied on the system in both the localized and non-localized cases. Due to the way cost functions are defined, each agent has a negligible influence on the system as a whole as $N \to \infty$. In the infinite population limit, a Nash Equilibrium exists (to be proven) where each agent is playing against a mass which is represented by the Mean Field which is driven by the collection of the individual asymptotically negligible influences of each agent. In effect, each agent becomes a generic agent. The dynamics of the Mean Field density (assumed to exist) as well as the value function and best response controls of such a generic agent can all be found from the coupled loop of MFG equations consisting of the MFG Fokker-Planck-Kolmogorov (MFG FPK) and MFG Hamilton-Jacobi-Bellman (MFG HJB) equations where it is assumed that the initial Mean Field density is known to all agents. For the MFG PDEs in the following analysis we assume a state domain of $D$, i.e. $\theta \in D$.

### 3.7.1 Models Without Localized Cost or Agent Motion

#### Infinite Population Limit and Generic Agent Dynamics and Costs

In order to develop the MFG equations, one needs to first discuss the dynamics and costs of the generic agent. The dynamics of the generic agent in the infinite population case are identical to the finite population dynamics and can be seen in (3.12). This is due to the fact that the finite population dynamics of each agent in this problem are local and do not depend on other agent states, controls or the number of agents in the system. Now developing the cost functions, the cost-to-go of the generic agent $i$ in the infinite population limit is given by

$$J_i^{\infty}(s,u,\tilde{\theta}_i) \triangleq \lim_{N\to\infty} E\left[\int_s^T \left(-\frac{p_{out}^i(t)}{\frac{1}{N}\sum_{k=1}^N p_{out}^k(t)+\eta} + p_{in}^i(t)\right) dt \middle| \theta_i(s)=\tilde{\theta}_i\right] \quad (3.26)$$

$$= E\left[\int_s^T \left(-\frac{p_{out}^i(t)}{\int_{\Omega_\theta} p_{out} f_{\mu_t}(\theta) d\theta+\eta} + p_{in}^i(t)\right) dt \middle| \theta_i(s)=\tilde{\theta}_i\right] \quad (3.27)$$

where $\theta = \begin{pmatrix}\beta & p_{in} & p_{out}\end{pmatrix}^T$, $f_{\mu_t}(\theta)$ is the probability density function of the Mean Field (assumed to exist) at time $t \in [0,T]$ and $\Omega_\theta = \Omega_\beta \times \Omega_{p_{in}} \times \Omega_{p_{out}}$ is the support set of $f_{\mu_t}$.

Given the agent dynamics in (3.12) and cost functions (3.20) and (3.27) (in the finite and infinite populations respectively) it may be verified that assumptions (**A1**)-(**A7**) and (**H4**) in [16] hold and therefore there exists a unique solution $(\theta^1(\cdot),...,\theta^N(\cdot))$ to the set of SDEs given by (3.12), $1 \le i \le N$.

The value function of generic agent $i$ is then defined as:

$$V_i(s,\tilde{\theta}_i) = \inf_{u\in U} J_i^{\infty}(s,u,\tilde{\theta}_i) \quad (3.28)$$

where here $u \in [-1,1]$ corresponds to the control $u_{p_{in}}$ of the transmit power of the generic agent.

### The MFG HJB Equation and Best Response Control

Given the Mean Field density, $f_{\mu_t}(\theta)$ and following from the costs developed for the generic agent in (3.27), the MFG HJB equation of the generic agent is given by

$$\begin{aligned}-\frac{\partial V}{\partial t} &= -\frac{p_{out}}{\int_{\Omega_\theta} p_{out} f_{\mu_t}(\theta)d\theta+\eta} + p_{in} + \frac{\partial V}{\partial p_{out}}\left(\frac{\sigma_{p_{out}}^2}{2\epsilon}\right)\left(1-\frac{p_{out}}{e^{\beta}p_{in}+\nu}\right) \quad (3.29)\\ &+ \frac{\partial V}{\partial \beta}(-a(\beta+b)) + \frac{\partial^2 V}{\partial \beta^2}\frac{\sigma_\beta^2}{2} + \frac{\partial^2 V}{\partial p_{in}^2}\frac{\sigma_{p_{in}}^2}{2} + \frac{\partial^2 V}{\partial p_{out}^2}\frac{\sigma_{p_{out}}^2}{2\epsilon}p_{out}\\ &+ \inf_{u_{p_{in}}\in U_{p_{in}}}\{H(u_{p_{in}})\}, \qquad V(T,\theta)=0, \quad (t,\theta)\in[0,T]\times D\end{aligned}$$

where $H(u_{p_{in}}) = u_{p_{in}} \frac{\partial V}{\partial p_{in}}$. From the infimized Hamiltonian in (3.29) the best response control of the generic agent is given by

$$u^*_{p_{in}} = \arg \inf_{u_{p_{in}} \in U_{p_{in}}} \{H(u_{p_{in}})\} = \arg \min_{u_{p_{in}} \in U_{p_{in}}} \left\{ u_{p_{in}} \frac{\partial V}{\partial p_{in}} \right\} \tag{3.30}$$

assuming the minimum exists. Because $U_{p_{in}} = [-1, 1]$, it follows that

$$u^*_{p_{in}} = -sign \left\{ \frac{\partial V}{\partial p_{in}} \right\} \tag{3.31}$$

The MFG HJB equation therefore reduces to

$$\begin{aligned} -\frac{\partial V}{\partial t} &= -\frac{p_{out}}{\int_{\Omega_\theta} p_{out} f_{\mu_t}(\theta) d\theta + \eta} + p_{in} + \frac{\partial V}{\partial p_{out}} \left( \frac{\sigma^2_{p_{out}}}{2\epsilon} \right) \left( 1 - \frac{p_{out}}{e^\beta p_{in} + \nu} \right) \\ &+ \frac{\partial V}{\partial \beta}(-a(\beta + b)) + \frac{\partial^2 V}{\partial \beta^2} \frac{\sigma^2_\beta}{2} + \frac{\partial^2 V}{\partial p^2_{in}} \frac{\sigma^2_{p_{in}}}{2} + \frac{\partial^2 V}{\partial p^2_{out}} \frac{\sigma^2_{p_{out}}}{2\epsilon} p_{out} \\ &- sign \left\{ \frac{\partial V}{\partial p_{in}} \right\}, \qquad V(T, \theta) = 0, \quad (t, \theta) \in [0, T] \times D \end{aligned} \tag{3.32}$$

### The MFG FPK Equation

Given the best response control $u$ of the generic agent, the Mean Field dynamics are given by the following MFG FPK equation,

$$\begin{aligned} \frac{\partial f_{\mu_t}}{\partial t} &= -\frac{\partial}{\partial \beta} [-a(\beta + b) f_{\mu_t}] - \frac{\partial}{\partial p_{in}} [u f_{\mu_t}] - \frac{\partial}{\partial p_{out}} \left[ \frac{\sigma^2_{p_{out}}}{2\epsilon} \left( 1 - \frac{p_{out}}{e^\beta p_{in} + \nu} \right) f_{\mu_t} \right] \\ &+ \frac{\partial^2}{\partial \beta^2} \left[ \frac{\sigma^2_\beta}{2} f_{\mu_t} \right] + \frac{\partial^2}{\partial p^2_{in}} \left[ \frac{\sigma^2_{p_{in}}}{2} f_{\mu_t} \right] + \frac{\partial^2}{\partial p^2_{out}} \left[ \frac{\sigma^2_{p_{out}}}{2\epsilon} p_{out} f_{\mu_t} \right], \qquad (t, \theta) \in [0, T] \times D \end{aligned} \tag{3.33}$$

### The MFG Loop

We now define the MFG Loop of the non-localized problem to be the set of coupled MFG equations, namely the MFG HJB, MFG best response and MFG FPK equations given by (3.29), (3.31) and (3.33) respectively. The MFG Loop is depicted in

(3.34) below.

$$\begin{tikzcd} f_{\mu_t}(\theta) \arrow[rr, "(3.29)"] & & V(t,\theta) \arrow[dl, "(3.31)"] \\ & u^*(t,\theta) \arrow[ul, "(3.33)"] & \end{tikzcd} \tag{3.34}$$

### 3.7.2 Models With Localized Cost and Agent Motion

#### Infinite Population Limit and Generic Agent Dynamics and Costs

We now follow the same idea as Section 3.7.1 to develop the analogous infinite population MFG equations for the optimization problem with localized costs and agent motion. The dynamics of the generic agent, as in the previous case are identical to the relevant dynamics of each agent in the finite population system namely driven by (3.13). The cost-to-go of a given agent $i$ in the infinite population limit is given by

$$J_i^{\infty}(s,u,\tilde{\theta}_i) \triangleq \lim_{N\to\infty} E\left[\int_s^T \left(-\frac{e^{-||x^i(t)-x^b||^2} p^i_{out}(t)}{\frac{1}{N}\sum_{k=1}^N e^{-||x^k(t)-x^b||^2} p^k_{out}(t)+\eta} + p^i_{in}(t)\right) dt \middle| \theta_i(s)=\tilde{\theta}_i\right] \tag{3.35}$$

$$= E\left[\int_s^T \left(-\frac{e^{-||x^i(t)-x^b||^2} p^i_{out}(t)}{\int_{\Omega_\theta} e^{-||x-x^b||^2} p_{out} f_{\mu_t}(\theta) d\theta+\eta} + p^i_{in}(t)\right) dt \middle| \theta_i(s)=\tilde{\theta}_i\right] \tag{3.36}$$

where $\theta = \begin{pmatrix}\beta & p_{in} & p_{out} & x_1 & x_2\end{pmatrix}^T$, $f_{\mu_t}(\theta)$ is the probability density function of the Mean Field (assumed to exist) at time $t$ and $\Omega_\theta = \Omega_\beta \times \Omega_{p_{in}} \times \Omega_{p_{out}} \times \Omega_{x_1} \times \Omega_{x_2}$ is the support set of $f_{\mu_t}$.

Given the agent dynamics in (3.13) and cost functions (3.25) and (3.36) (in the finite and infinite populations respectively) it may be verified that assumptions (**A1**)-(**A7**) and (**H4**) in [16] hold and therefore there exists a unique solution $(\theta^1(\cdot), ..., \theta^N(\cdot))$ to the set of SDEs given by (3.13), $1 \le i \le N$.

The value function of agent $i$ is then defined as

$$V_i(s, \tilde{\theta}_i) = \inf_{u \in U} J_i^{\infty}(s, u, \tilde{\theta}_i) \tag{3.37}$$

where here $u = \begin{pmatrix} u_{p_{in}} & u_{x_1} & u_{x_2} \end{pmatrix}^T$ corresponds to the controls $u_{p_{in}}, u_{x_1}, u_{x_2} \in [-1, 1]$ of agent transmit power and position in each dimension of two-dimensional space respectively.

### The MFG HJB Equation and Best Response Control

Given the Mean Field density, $f_{\mu_t}(\theta)$, and following from the costs of the generic agent in (3.36), the MFG HJB equation of the generic agent is given by

$$\begin{aligned}
-\frac{\partial V}{\partial t} &= -\frac{e^{-||x-x^b||^2} p_{out}}{\int_{\Omega_\theta} e^{-||x-x^b||^2} p_{out} f_{\mu_t}(\theta) d\theta + \eta} + p_{in} + \frac{\partial V}{\partial p_{out}} \left( \frac{\sigma_{p_{out}}^2}{2\epsilon} \right) \left( 1 - \frac{p_{out}}{e^\beta p_{in} + \nu} \right) \\
&\quad + \frac{\partial V}{\partial \beta}(-a(\beta + b)) + \frac{\partial^2 V}{\partial \beta^2} \frac{\sigma_\beta^2}{2} + \frac{\partial^2 V}{\partial p_{in}^2} \frac{\sigma_{p_{in}}^2}{2} + \frac{\partial^2 V}{\partial p_{out}^2} \frac{\sigma_{p_{out}}^2}{2\epsilon} p_{out} + \frac{\partial^2 V}{\partial x_1^2} \frac{\sigma_{x_1}^2}{2} \\
&\quad + \frac{\partial^2 V}{\partial x_2^2} \frac{\sigma_{x_2}^2}{2} + \inf_{u_{p_{in}}, u_{x_1}, u_{x_2} \in U} \{ H(u_{p_{in}}, u_{x_1}, u_{x_2}) \}, \\
&\quad V(T, \theta) = 0, \quad (t, \theta) \in [0, T] \times D
\end{aligned} \tag{3.38}$$

where $H(u_{p_{in}}, u_{x_1}, u_{x_2}) = u_{p_{in}} \frac{\partial V}{\partial p_{in}} + u_{x_1} \frac{\partial V}{\partial x_1} + u_{x_2} \frac{\partial V}{\partial x_2}$. From the infimized Hamiltonian in (3.38), the best response control of the generic agent is given by

$$u_{p_{in}}^* = -sign \left\{ \frac{\partial V}{\partial p_{in}} \right\}, u_{x_1}^* = -sign \left\{ \frac{\partial V}{\partial x_1} \right\}, u_{x_2}^* = -sign \left\{ \frac{\partial V}{\partial x_2} \right\} \tag{3.39}$$

The MFG HJB equation therefore reduces to

$$
\begin{aligned}
-\frac{\partial V}{\partial t} &= -\frac{e^{-||x-x^b||^2} p_{out}}{\int_{\Omega_\theta} e^{-||x-x^b||^2} p_{out} f_{\mu_t}(\theta) d\theta + \eta} + p_{in} + \frac{\partial V}{\partial p_{out}} \left( \frac{\sigma^2_{p_{out}}}{2\epsilon} \right) \left( 1 - \frac{p_{out}}{e^{\beta} p_{in} + \nu} \right) \qquad (3.40) \\
&+ \frac{\partial V}{\partial \beta}(-a(\beta + b)) + \frac{\partial^2 V}{\partial \beta^2} \frac{\sigma^2_{\beta}}{2} + \frac{\partial^2 V}{\partial p_{in}^2} \frac{\sigma^2_{p_{in}}}{2} + \frac{\partial^2 V}{\partial p_{out}^2} \frac{\sigma^2_{p_{out}}}{2\epsilon} p_{out} + \frac{\partial^2 V}{\partial x_1^2} \frac{\sigma^2_{x_1}}{2} \\
&+ \frac{\partial^2 V}{\partial x_2^2} \frac{\sigma^2_{x_2}}{2} - sign \left\{ \frac{\partial V}{\partial p_{in}} \right\} - sign \left\{ \frac{\partial V}{\partial x_1} \right\} - sign \left\{ \frac{\partial V}{\partial x_2} \right\}, \\
&V(T, \theta) = 0, \quad (t, \theta) \in [0, T] \times D
\end{aligned}
$$

**The MFG FPK Equation**

Given the best response control $u$ of the generic agent, as well as the state dynamics of the generic agent, the Mean Field dynamics follow the MFG FPK equation,

$$
\begin{aligned}
\frac{\partial f_{\mu_t}}{\partial t} &= -\frac{\partial}{\partial \beta} \left[ -a(\beta + b) f_{\mu_t} \right] - \frac{\partial}{\partial p_{in}} \left[ u_{p_{in}} f_{\mu_t} \right] - \frac{\partial}{\partial p_{out}} \left[ \frac{\sigma^2_{p_{out}}}{2\epsilon} \left( 1 - \frac{p_{out}}{e^{\beta} p_{in} + \nu} \right) f_{\mu_t} \right] \qquad (3.41) \\
&- \frac{\partial}{\partial x_1} \left[ u_{x_1} f_{\mu_t} \right] - \frac{\partial}{\partial x_2} \left[ u_{x_2} f_{\mu_t} \right] + \frac{\partial^2}{\partial \beta^2} \left[ \frac{\sigma^2_{\beta}}{2} f_{\mu_t} \right] + \frac{\partial^2}{\partial p_{in}^2} \left[ \frac{\sigma^2_{p_{in}}}{2} f_{\mu_t} \right] \\
&+ \frac{\partial^2}{\partial p_{out}^2} \left[ \frac{\sigma^2_{p_{out}}}{2\epsilon} p_{out} f_{\mu_t} \right] + \frac{\partial^2}{\partial x_1^2} \left[ \frac{\sigma^2_{x_1}}{2} f_{\mu_t} \right] + \frac{\partial^2}{\partial x_2^2} \left[ \frac{\sigma^2_{x_2}}{2} f_{\mu_t} \right], \quad (t, \theta) \in [0, T] \times D
\end{aligned}
$$

**The MFG Loop**

Similarly to the MFG Loop in the non-localized problem we now define the MFG Loop of the localized problem to be the set of coupled equations given by (3.38), (3.39) and (3.41). The MFG Loop is depicted in (3.42) below.

$$
\begin{tikzcd}
f_{\mu_t}(\theta) \arrow[rr, "(3.38)"] & & V(t,\theta) \arrow[dl, "(3.39)"] \\
& u^*(t,\theta) \arrow[ul, "(3.41)"] &
\end{tikzcd}
\qquad (3.42)
$$

### 3.7.3 Existence and Uniqueness of Solutions of the MFG PDEs

For each of the non-localized and localized problems we now provide an analysis of the existence and uniqueness of solutions of the MFG PDEs separately before discussing the existence and uniqueness of a solution of the nonlinear MFG Loop in Section 3.7.4.

#### General Existence and Uniqueness of Solutions of FPK Equations

We begin by presenting the general results on second order parabolic PDEs as described in Chapter 7 of [38] and as used similarly in [17, 18]. The $H_0^1$, $H^{-1}$, and $H^2$ spaces described below denote the Sobolev spaces of relevant order. For more information on their definitions as well as the definition of weak derivatives the reader is referred to Appendix B. Consider PDEs of the form

$$\frac{\partial \mu}{\partial t} + \Psi\mu = f \text{ in } D_T \tag{3.43}$$

$$\mu = 0 \text{ on } \partial D \times [0, T] \tag{3.44}$$

$$\mu = g \text{ on } D \times \{t = 0\} \tag{3.45}$$

where $D$ is an open bounded subset of $\mathbb{R}^n$, $D_T = D \times (0, T]$, $T > 0$, $f : D_T \to \mathbb{R}$ and $g : D \to \mathbb{R}$ are given and $\mu : \overline{D}_T \to \mathbb{R}$ is the unknown. Here the operator $\Psi$ is defined as

$$\Psi\mu = -\sum_{i,j=1}^{n}((a^{ij}(x,t)\mu_{x_i})_{x_j} + \sum_{i=1}^{n} b^i(x,t)\mu_{x_i} + c(x,t)\mu \tag{3.46}$$

Note that FPK equations naturally fit this form. Let the "compatibility conditions" denote those indicated in [38] Chapter 7 Theorem 6. Summarizing Theorems 3, 4, 5, 7 in [38] Chapter 7 the following compendium theorem is obtained.

**Theorem 1.** *Existence and Uniqueness of Solutions of Parabolic PDEs*
*Assume $a^{ij}$ is positive semi-definite, and $a^{ij}, b^i, c \in L^\infty(D_T)$ for all choices of indices and $f, g \in L^2(D_T)$. Then, there exists a unique weak solution $\mu$ to the parabolic equa-*

*tion (3.43)-(3.45) which satisfies* $\mu \in L^2(0,T;H_0^1(D))$ *and* $\mu' \in L^2(0,T;H^{-1}(D))$. *If, in addition,* $a^{ij}, b^i, c$ *are smooth on* $\overline{D}$ *and do not depend on* $t$ *and,* $g \in H_0^1(D)$ *and* $f \in L^2(0,T;L^2(D))$, *then* $\mu \in L^2(0,T;H^2(D)) \cap L^\infty(0,T;H_0^1(D))$ *and* $\mu' \in L^2(0,T;L^2(D))$. *If the compatibility conditions hold and,* $g \in C^\infty(\overline{D})$ *and* $f \in C^\infty(\overline{D_T})$ *then* $\mu \in C^\infty(\overline{D_T})$.

**General Existence and Uniqueness of Solutions of HJB Equations**

The following analysis is developed with reference to Chapter 4 of [39]. Consider a stochastic controlled system:

$$dx(t) = b(t,x(t),u(t))dt + \sigma(t,x(t),u(t))dW(t),\ t \in [s,T], \tag{3.47}$$

$$x(s) = y \tag{3.48}$$

with cost functional

$$J(s,y;u(\cdot)) = E\left\{\int_s^T f(t,x(t),u(t))dt + h(x(T))\right\} \tag{3.49}$$

and value function

$$V(s,y) = \inf_{u(\cdot)\in U[s,T]} J(s,y;u(\cdot)), \forall (s,y) \in [0,T) \times \mathbb{R}^n \tag{3.50}$$

Consider further the following Hamilton Jacobi Bellman equation

$$-v_t + \sup_{u\in U} G(t,x,u,-v_x,-v_{xx}) = 0, (t,x) \in [0,T) \times \mathbb{R}^n, \tag{3.51}$$

$$v|_{t=T} = h(x), x \in \mathbb{R}^n \tag{3.52}$$

where

$$G(t,x,u,p,P) \triangleq \frac{1}{2} tr(P\sigma(t,x,u)\sigma(t,x,u)^T) + \langle p, b(t,x,u)\rangle - f(t,x,u) \tag{3.53}$$

Two assumptions are now defined:

(**S1**) The control space $U$ is a compact subset of $\mathbb{R}^n$ and $T > 0$.

(**S2**) The maps $b : [0,T] \times \mathbb{R}^n \times U \to \mathbb{R}^n, \sigma : [0,T] \times \mathbb{R}^n \times U \to \mathbb{R}^{n\times m}, f : [0,T] \times \mathbb{R}^n \times U \to \mathbb{R}$ and $h : \mathbb{R}^n \to \mathbb{R}$ are uniformly continuous and uniformly Lipschitz in $x$.

Theorems 5.2, 6.1 in Chapter 4 [39] taken together yield the following result.

**Theorem 2.** *Existence and Uniqueness of Viscosity Solutions of HJB Equations. Let (**S1**) and (**S2**) hold. Then there exists a unique viscosity solution $v$ to the HJB equation (3.51), (3.52) and that solution is equal to the value function $V$ of the stochastic control problem. Furthermore if $v \in C^{1,2}([0,T] \times \mathbb{R}^n)$ then the viscosity solution is a classical solution.*

The following proposition is now presented which is used in the analysis of the MFG HJB equations.

**Proposition 1.** *[39] Chapter 4, Proposition 4.1.*
*Suppose (**S1**)-(**S2**) hold for $(b^\xi, \sigma^\xi, f^\xi, h^\xi)$ with $\xi \in [0,1]$ and $b^0 = b, \sigma^0 = \sigma, f^0 = f, h^0 = h$. Suppose further that $\lim_{\xi\to 0} |\phi^\xi(t,x,u) - \phi(t,x,u)| = 0$, uniformly in $(t,u) \in [0,T] \times U$ and $x$ in compact sets of $\mathcal{R}^n$, where $\phi^\xi = b^\xi, \sigma^\xi, f^\xi, h^\xi$. Then, $\lim_{\xi\to 0} V^\xi(s,y) = V(s,y)$.*

### Existence and Uniqueness of Solutions of the CDMA MFG FPK and MFG HJB Equations

We now consider the existence and uniqueness of solutions of the MFG PDEs separately. In particular, we address the existence and uniqueness of a solution of the MFG HJB equations (in both problems) given the Mean Field dynamics and we then address the existence and uniqueness of a solution of the MFG FPK equations (in both problems) given the optimal generic agent controls.

**Models Without Localized Cost or Agent Motion**

Let $D = (\beta^{min}, \beta^{max}) \times (0, p_{in}^{max}) \times (0, p_{out}^{max})$ be the bounded open domain over which we are considering existence and uniqueness of solutions of the MFG PDEs. We begin with the existence and uniqueness of a solution of the MFG HJB equation. Considering the dynamics of the generic agent, the following result is obtained.

**Proposition 2.** *There exists a unique viscosity solution $v$ to (3.29) which is equal to the value function $V$ in (3.28). Furthermore the value function is linearly bounded and uniformly Lipschitz with respect to state variables.*

*Proof.* Referring to the notation used for Theorem 2 we have for this problem,

$$b(t, x, u) = \begin{pmatrix} -a(\beta(t) + b) \\ u_{p_{in}}(t) \\ \frac{1}{\epsilon}\frac{(\sigma_{p_{out}})^2}{2}\left(1 - \frac{p_{out}(t)}{e^{\beta(t)}p_{in}(t)+\nu}\right) \end{pmatrix} \tag{3.54}$$

and

$$\sigma(t, x, u) = \begin{pmatrix} \sigma_\beta & 0 & 0 \\ 0 & \sigma_{p_{in}} & 0 \\ 0 & 0 & \frac{1}{\sqrt{\epsilon}}\sigma_{p_{out}}\sqrt{p_{out}(t)} \end{pmatrix} \tag{3.55}$$

and the MFG HJB equation (3.29). Consider now the perturbed dynamics of the generic agent using a small positive quantity $\xi$, $0 < \xi << 1$ and consider $\sigma^\xi$ defined below

$$\sigma^\xi(t, x, u) = \begin{pmatrix} \sigma_\beta & 0 & 0 \\ 0 & \sigma_{p_{in}} & 0 \\ 0 & 0 & \frac{1}{\sqrt{\epsilon}}\sigma_{p_{out}}\sqrt{p_{out}(t) + \xi} \end{pmatrix} \tag{3.56}$$

Considering the perturbed system which is identical to the original system except for the replacement of $\sigma^\xi(t, x, u)$ for $\sigma(t, x, u)$, it can be shown that (**S1**) and (**S2**) are satisfied on $D$. Therefore, by Theorem 2, there exists a unique viscosity solution $v^\xi$ to the perturbed system MFG HJB equation and that solution is equal to the value function $V^{\xi}(s, y)$ of the perturbed stochastic control problem, which is linearly bounded and uniformly Lipschitz in state variables. Furthermore by Proposition 1, since $\lim_{\xi \to 0} \sigma^{\xi}(t, x, u) = \sigma(t, x, u)$ uniformly, it follows that $\lim_{\xi \to 0} V^{\xi}(s, y) = V(s, y)$ which is the value function of the original unperturbed system, completing the proof. □

So, for the rest of the work it is assumed that a unique smooth classical solution exists for the MFG HJB equation (3.29) and that solution is equal to the value function (3.28).

For the existence and uniqueness of a solution of the MFG FPK equation, the following result is obtained.

**Proposition 3.** *Let $f_{\mu_0} \in C^{\infty}(\overline{D})$. Then, there exists a unique weak solution $f_{\mu_t}$ to (3.33). Further, $f_{\mu_t} \in C^{\infty}(\overline{D_T})$.*

*Proof.* Consider the alternate form of (3.33),

$$\begin{aligned} \frac{\partial f_{\mu_t}}{\partial t} = &-\frac{\partial}{\partial \beta}\left(-\frac{\sigma_{\beta}^2}{2}\frac{\partial f_{\mu_t}}{\partial \beta}\right) - \frac{\partial}{\partial p_{in}}\left(-\frac{\sigma_{p_{in}}^2}{2}\frac{\partial f_{\mu_t}}{\partial p_{in}}\right) - \frac{\partial}{\partial p_{out}}\left(-\frac{\sigma_{p_{out}}^2}{2\epsilon}p_{out}\frac{\partial f_{\mu_t}}{\partial p_{out}}\right) \\ &+ a(\beta + b)\frac{\partial f_{\mu_t}}{\partial \beta} + (-u_{p_{in}})\frac{\partial f_{\mu_t}}{\partial p_{in}} + \left(\frac{\sigma_{p_{out}}^2}{2\epsilon}\frac{p_{out}}{e^{\beta}p_{in} + \nu}\right)\frac{\partial f_{\mu_t}}{\partial p_{out}} \\ &+ \left(a + \frac{\sigma_{p_{out}}^2}{2\epsilon}\frac{1}{e^{\beta}p_{in} + \nu}\right) f_{\mu_t}, \qquad (t, \theta) \in [0, T] \times D \end{aligned} \tag{3.57}$$

On $D$, it is clear that $a^{ij}, b^i, c \in L^{\infty}(D_T)$ for all choices of indices where $a^{ij}, b^i, c$ are defined in Theorem 1. Furthermore, $a^{ij}, b^i, c$ are all smooth on $\overline{D}$ and do not depend on time. Also $f = 0 \Rightarrow f \in L^2(D_T)$ and $f \in C^{\infty}(\overline{D_T})$. Therefore, by Theorem 1, if $g = f_{\mu_0} \in C^{\infty}(\overline{D})$ and compatibility conditions hold, there exists a unique weak solution to the MFG FPK equation and $f_{\mu_t} \in C^{\infty}(\overline{D_T})$. □

**Models With Localized Cost and Agent Motion**

We now present theorems for the existence and uniqueness of solutions of the MFG HJB and MFG FPK equations in the case of localized cost and agent motion. The proofs are almost identical to those in the previous section and are therefore omitted for brevity. Let $D = (\beta^{min}, \beta^{max}) \times (0, p_{in}^{max}) \times (0, p_{out}^{max}) \times (x_1^{min}, x_1^{max}) \times (x_2^{min}, x_2^{max})$ be the open bounded domain of interest.

**Proposition 4.** *There exists a unique viscosity solution $v$ to (3.38) which is equal to the value function $V$ in (3.37). Furthermore the value function is linearly bounded and uniformly Lipschitz with respect to state variables.*

For the rest of the work it is assumed that a unique smooth classical solution exists for the MFG HJB equation (3.38) and that solution is equal to the value function (3.37). For the MFG FPK equation the following result is obtained.

**Proposition 5.** *Let $f_{\mu_0} \in C^\infty(\overline{D})$. Then there exists a unique weak solution $f_{\mu_t}$ to (3.41). Further, $f_{\mu_t} \in C^\infty(\overline{D_T})$.*

### 3.7.4 Existence and Uniqueness of Solutions of the MFG Loop

It has been shown that the MFG HJB and MFG FPK equations of both CDMA problems admit unique solutions separately. We now discuss existence and uniqueness of solutions of the nonlinear MFG Loops (3.34), (3.42) of the non-localized and localized problems respectively. The approach taken here is to apply the Contraction Principle argument from [16] to the MFG PDEs and best response controls.

Conditions are now described under which the loop has a unique solution, assuming that the MFG FPK and MFG HJB equations admit unique solutions separately. Consider the following assumptions (**H1**)-(**H6**),

(**H1**) The control value space $U$ is a compact subset of $\mathbb{R}^m$ and the final time $T$ satisfies $0 < T < \infty$.

(**H2**) The dynamics governing the states are smooth and together with their derivatives are uniformly Lipschitz in state variables and controls.

(**H3**) For any given smooth Mean Field density $f_{\mu_t}$, the loss function $L(\cdot)$ is smooth and together with its derivatives is uniformly Lipschitz in state variables.

(**H4**) The value function $V(\cdot)$ lies in $C^{1,2}[0,T]$.

(**H5**) The infimization operation in the Hamiltonian yields a unique solution continuous and uniformly Lipschitz in state variables.

(**H6**) The loop gain operator in the MFG Loop has Wasserstein norm strictly less than 1 on the space of solutions lying in $L^2 \cap L^\infty$.

We present the following theorem for general nonlinear MFG theory.

**Theorem 3.** *Contraction Theorem ([10]).*
*Assume (***H1***) to (***H6***) are satisfied for appropriately constrained parameter values and also assume that the MFG HJB and MFG FPK equations have unique solutions separately. Then there exists a contraction constant for which the MFG Loop converges.*

Following from Theorem 3 the following result is obtained

**Proposition 6.** *There exists a unique solution to each MFG Loop (3.34), (3.42) of the non-localized and localized problems respectively.*

The proof follows directly from the fact that assumptions (**H1**) - (**H6**) are met. The MFG Loop therefore yields a unique solution providing the value function $V(\cdot)$, the Mean Field density $f_{\mu_t}(\cdot)$ and the resulting optimal control strategies of the generic agent. These optimal controls form a unique Nash Equilibrium strategy set in the infinite population system. Given the applicability, in this case, of the contraction principle, one can approximately solve the problem by applying numerical methods and computation which is an important part of this work and will be discussed in Chapter 4.

### 3.7.5 Finite Population Implications of $\epsilon$-Nash Equilibria

In the above sections, agent controls and Mean Field dynamics are considered for the limiting infinite population system. In the presented problem, though there are a large number of agents in the network, there is a distinction between the infinite population continuum and the actual physical state of the system. A key aspect of MFG analysis is that if each agent assumes an infinite population with Mean Field describing the generic agent and if each agent then applies MFG optimal controls for the infinite population system, the controls chosen will result in an approximate Nash equilibrium or $\epsilon$-Nash equilibrium in the original finite population game.

**Theorem 4.** *MFG $\epsilon$-Nash Theorem ([10, 16])*
*Assume that all conditions of the MFG Nash Equilibrium Theorem hold and hence that the best response control laws $\mathcal{U}^\infty = \{u_0^i = u_0^i(t, x^i|\mu_t), 1 \leq i < \infty\}$ generating a Nash equilibrium for an infinite agent population system and associated performance functions exist. Then $\mathcal{U}^N = \{u_0^i = u_0^i(t, x^i|\mu_t), 1 \leq i \leq N\}$ yields a (strong) $\epsilon$-Nash equilibrium for all $\epsilon$, i.e. $\forall \epsilon > 0 \;\; \exists N(\epsilon) > 0 \;\; s.t. \;\; \forall N \geq N(\epsilon)$,*

$$J^i(u_0^i, u_0^{-i}) - \epsilon \leq \inf_{u^i \in \mathcal{U}} J^i(u^i, u_0^{-i}) \leq J^i(u_0^i, u_0^{-i})$$

*where $u^i \in \mathcal{U}$, the set of all past dependent controls of the form $u^i = u^i(t, x^i|\mu_t)$.*

Applying this theorem to the two CDMA optimization problems, it is therefore concluded that the infinite population MFG optimal controls result in an $\epsilon$-Nash equilibrium in the actual finite population systems.

# Chapter 4

# Numerical Investigations of CDMA Control Problems

In this chapter, numerical algorithms are provided for the solutions to the two CDMA network optimization problems in Chapter 3. In addition, these algorithms are verified through simulations in order to provide illustrative examples. The chapter is organized as follows. First, we provide the PDE discretization techniques used for the MFG HJB and MFG FPK equations as well as all boundary conditions. Then, following closely [17, 18], two numerical algorithms are provided. The first computes the solution of the MFG Loop resulting in the Mean Field density dynamics as well as the value function and optimal controls of the generic agent. The second algorithm uses the MFG Loop solution in order to simulate particular sample paths of system agent states, costs and controls which are applying the MFG optimal controls as computed in the first algorithm. The final part of this chapter presents certain chosen simulations for illustration.

## 4.1 PDE and State Discretization Techniques

In order to apply numerical investigations of the two MFG CDMA problems and to compute the convergent solutions of the MFG Loops, one must first discretize the relevant equations. In this work, a finite difference method is used [40]. We transform the MFG HJB and MFG FPK equations into relevant difference equations and apply numerical iterations to approximate their curves in time and their state domain spaces.

### 4.1.1 Boundary Conditions and State Discretization

First, the domains of the agent state variables are restricted to a discrete grid in $\mathbb{R}^3$ or $\mathbb{R}^5$ for the case without and with agent motion respectively. The domain of states $\beta$, $p_{in}$, $p_{out}$, $x_1$, $x_2$ are bounded to stay within $[\beta^{min}, \beta^{max}]$, $[0, p_{in}^{max}]$, $[0, p_{out}^{max}]$, $[x_1^{min}, x_1^{max}]$, $[x_2^{min}, x_2^{max}]$ respectively where each point in the restricted domain of state component $z$ is given by $\{z_i = z^{min} + i * \Delta z\}$ for all $0 \leq i \leq N_z - 1$ where $N_z$ is the number of discrete state values the variable $z$ can take and $\Delta z$ is the constant spacing between each point of the discretized domain of state variable $z$. Time while already being bounded to the domain of $[0, T]$ has been discretized to points $t_n$, $0 \leq n \leq N_t$, where $t_n = n * \Delta t$, $\Delta t$ is the uniform time step, $N_t$ is the number of discrete time points.

### 4.1.2 PDE Discretization

We now define the methods used to approximate first and second order partial derivatives. Let $f(x_1, x_2, ...)$ be a function of multiple variables and let $x_1$ be the variable with respect to which we want to approximate the derivative of $f$. The first order derivative of $f$ with respect to $x_1$ is approximated as

$$\frac{\partial f(x_1, x_2, ...)}{\partial x_1} = \frac{f(x_1 + \Delta x_1, x_2, ...) - f(x_1, x_2, ...)}{\Delta x_1} \tag{4.1}$$

The first order partial derivatives with respect to the other variables $x_2, ...$ are approximated similarly. Further, the second order derivative of $f$ with respect to $x_1$ is approximated as

$$\frac{\partial^2 f(x_1, x_2, ...)}{\partial x_1^2} = \frac{f(x_1 + \Delta x_1, x_2, ...) - 2f(x_1, x_2, ...) + f(x_1 - \Delta x_1, x_2, ...)}{(\Delta x_1)^2} \tag{4.2}$$

and the second order partial derivatives with respect to other variables $x_2, ...$ are approximated similarly.

## 4.2 Numerical Algorithms for the Solution of the MFG Equations

Given the MFG Loop and following a similar idea to that of the work in [17, 18], the algorithms for the solution of the MFG equations are described below. A fixed point algorithm is first used to numerically compute the values of the Mean Field density, the value function and the best response controls of the generic agent for all times and discrete state values. The algorithm is shown below where $t$ and $\theta$ are understood to be discrete (after discretization) variables for times and states respectively. We present only the algorithm in the case without localized cost or agent motion, the inclusion of which merely involves the addition of two new discrete dimensions (namely one for each position dimension) as well as the solution of two additional discretized Hamiltonians corresponding to the latter two in (3.39) which are solved almost identically as the one presented.

**Data**: $f_{\mu_0}(\cdot)$ the initial Mean Field density

**Result**: $f_{\mu_t}(\cdot)$, $V(\cdot)$, $u^*(\cdot)$

$V^{<0>}(T,\theta) := 0$ for all $\theta$;

$u^{*<0>}(T,\theta) := -1$ for all $\theta$;

$f_{\mu_t}^{<-1>}(\theta) := \infty$ for all $t$ and $\theta$;

$i := 0$;

**while** $|{f_{\mu_t}}^{<i>}(\theta) - {f_{\mu_t}}^{<i-1>}(\theta)|_\infty > \epsilon_c$ **do**

Plug ${f_{\mu_t}}^{<i>}(\cdot)$ into the discretized MFG HJB equation and solve the equation in the backwards direction to update $V^{<i+1>}(t,\theta)$;

Use $V^{<i+1>}(\cdot)$ to find the best response controls $u^{*<i+1>}(t,\theta)$ from the minimization of the discretized Hamiltonian:

$$ {u_{p_{in}}}^{*<i+1>}(t,\theta) = -sign\left\{\frac{V^{<i+1>}(t,\beta,p_{in}+\Delta p_{in},p_{out}) - V^{<i+1>}(t,\beta,p_{in},p_{out})}{\Delta p_{in}}\right\} $$

Plug the best response controls $u^{*<i+1>}(\cdot)$ into the discretized MFG FPK equation and solve the equation in the forwards direction to update ${f_{\mu_t}}^{<i+1>}(\theta)$;

$i := i + 1$;

**end**

**Algorithm 1:** MFG PDE solver

Next, Algorithm 2 solves for a particular generic agent's state, controls and value function sample paths given the Mean Field triple $f_{\mu_t}(\cdot)$, $V(\cdot)$, $u^*(\cdot)$ determined from Algorithm 1.

**Data**: $f_{\mu_t}(\cdot)$, $V(\cdot)$, $u^*(\cdot)$, $\theta^i(0)$

**Result**: $V^i(t), \theta^i(t), u^{*i}(t)$ for all $t$

Generate all state Brownian Motions of generic agent $i$, $W^i(t)$;

**for** *each discrete time* $t$ **do**

Find the closest grid point $\overline{\theta}$ to $\theta^i(t)$ in the discretized state domain;

$V^i(t) := V(t, \overline{\theta})$;

Determine the best response control of the agent $u^*(t, \overline{\theta})$;

$u^i(t) := u^*(t, \overline{\theta})$;

Apply the control $u^i(t)$ and compute the next state value $\theta^i(t + \Delta t)$ by iterating the discretized agent state SDEs;

**end**

**Algorithm 2:** MFG sample path solver

## 4.3 Simulation Results of the System Without Agent Motion

Simulations of the CDMA optimization problem without agent motion or position state variables are now investigated. The SDE parameters are chosen to be $a = 0.1$, $b = 0.1$, $\sigma_\beta = 0.4$, $\sigma_{p_{in}} = 0.6$, $\sigma_{p_{out}} = 0.6$, $\nu = 0.1$. The noise power is chosen to be $\eta = 0.25$. The slow-fast parameter $\epsilon$ is given by $\epsilon = 0.01$. For the relevant discretization parameters, the final time is chosen to be $T = 1$ with $\Delta t = 0.003$. The domain is bounded by $\beta \in (\beta^{min}, \beta^{max}) = (-1, 1)$, $p_{in} \in (p_{in}^{min}, p_{in}^{max}) = (0, 3)$ and $p_{out} \in (p_{out}^{min}, p_{out}^{max}) = (0, 6)$. Also, it is set that $\Delta\beta = 0.1$, $\Delta p_{in} = 0.15$, $\Delta p_{out} = 0.3$. The initial Mean Field density $f_{\mu_0}$ is chosen to be a discretized approximation of the Gaussian distribution $\mathcal{N}\left(\begin{pmatrix} -0.3 \\ 2 \\ 2 \end{pmatrix}, \begin{pmatrix} 0.3 & 0 & 0 \\ 0 & 0.4 & 0 \\ 0 & 0 & 0.4 \end{pmatrix}\right)$.

A simulation of Algorithm 1 is first investigated where the MFG Loop is solved for the dynamics of the Mean Field density $f_{\mu_t}$ as well as the dynamics of the value function $V$ of the generic agent. The stopping condition is set to be $\epsilon_c = 0.0001$.

Fig. 4.1 shows the resulting joint marginal Mean Field density of state parameters $\beta$ and $p_{out}$ denoted as $f_{\mu_t}^{\beta,p_{out}}(\beta, p_{out})$ at the times $t \in \{0, 0.5, 0.75, 1\}$.

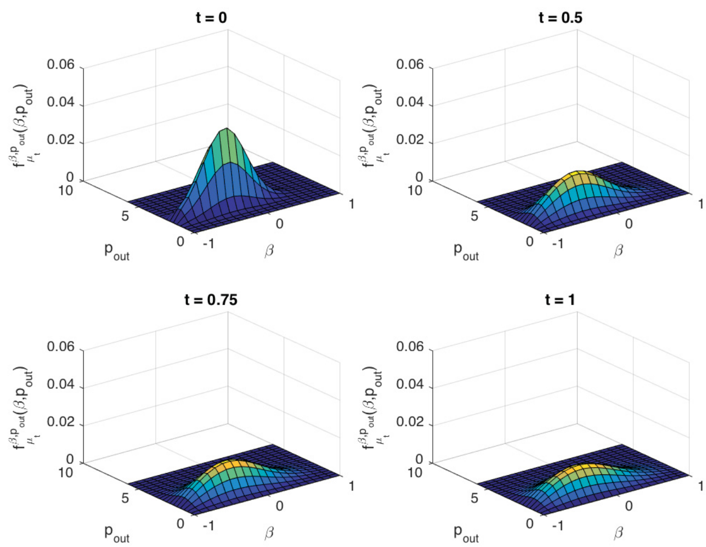


**Fig. 4.1** Dynamics of the marginal Mean Field density of $\beta$ and $p_{out}$

The corresponding "marginal" value function of the generic agent of state parameters $\beta$ and $p_{out}$ denoted as $V_{\beta,p_{out}}(t, \beta, p_{out})$ which is defined to be

$$V_{\beta,p_{out}}(t, \beta, p_{out}) = \int_{\Omega_{p_{in}}} V(t, \beta, p_{in}, p_{out}) f_{\mu_t}(\beta, p_{in}, p_{out}) dp_{in} \tag{4.3}$$

is given in Fig. 4.2 at the times $t \in \{0, 0.5, 0.75, 1\}$.

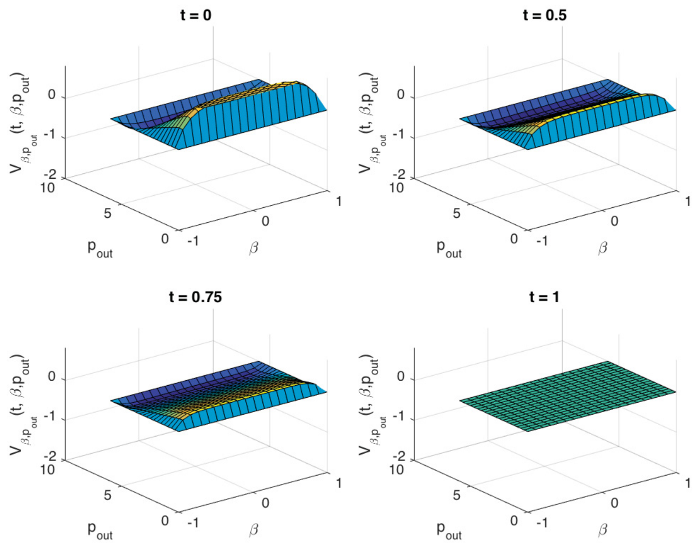


**Fig. 4.2** Dynamics of the value function of $\beta$ and $p_{out}$

Next, the dynamics in time of the marginal Mean Field densities $f_{\mu_t}^{\beta}(\beta)$, $f_{\mu_t}^{p_{in}}(p_{in})$, $f_{\mu_t}^{p_{out}}(p_{out})$, are shown in Fig. 4.3 to 4.5.

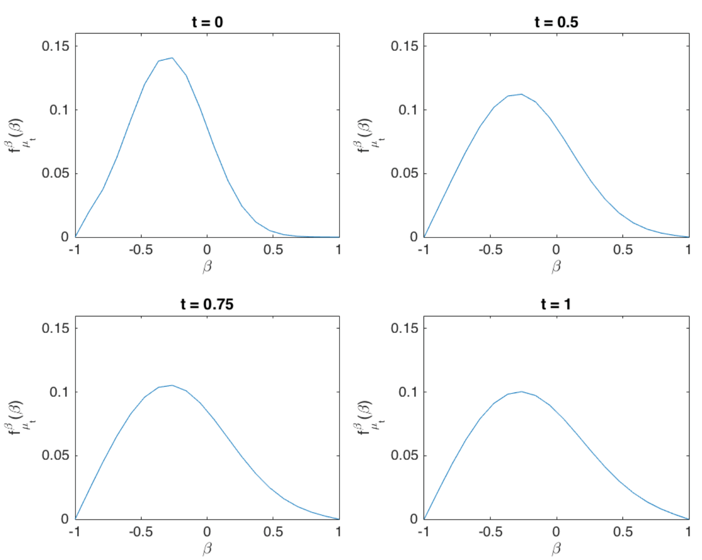


**Fig. 4.3** Dynamics of the marginal Mean Field density of $\beta$

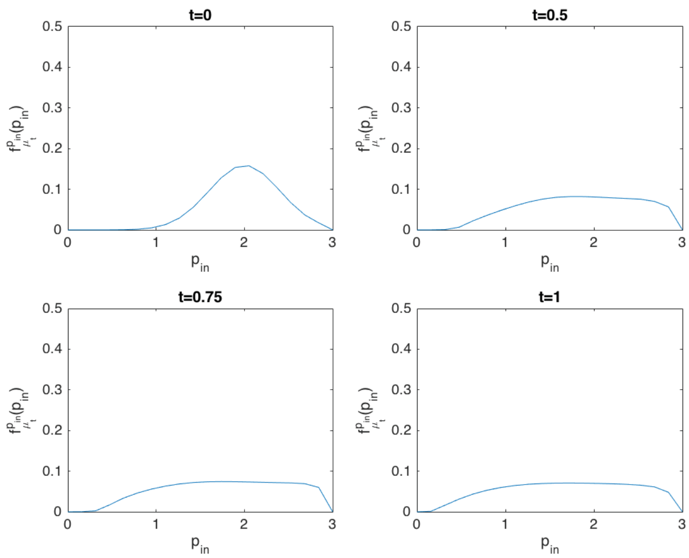


**Fig. 4.4** Dynamics of the marginal Mean Field density of $p_{in}$

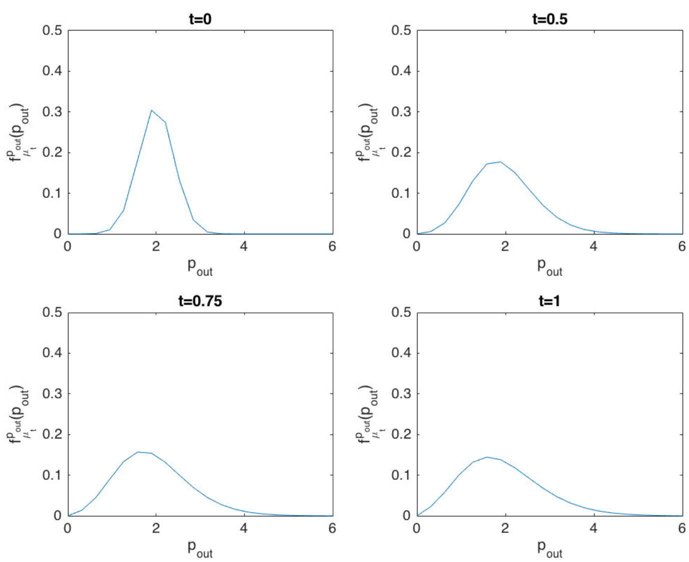


**Fig. 4.5** Dynamics of the marginal Mean Field density of $p_{out}$

In addition to the Mean Field PDE numerical investigations illustrated above, some investigations on particular sample path behaviour of a given agent in the system are considered, similar to those presented in [17, 18]. Fig. 4.6 shows the results of a simulation of Algorithm 2 with the same parameters mentioned at the beginning of the section as well as the initial conditions $\beta_0 = 0$, $(p_{in})_0 = 1.6$, $(p_{out})_0 = 1.8$. In particular, random sample path behaviour of each of the given agent's state variables, the agent's best response controls as determined by the infinite population MFG solution and the agent's value function are depicted.

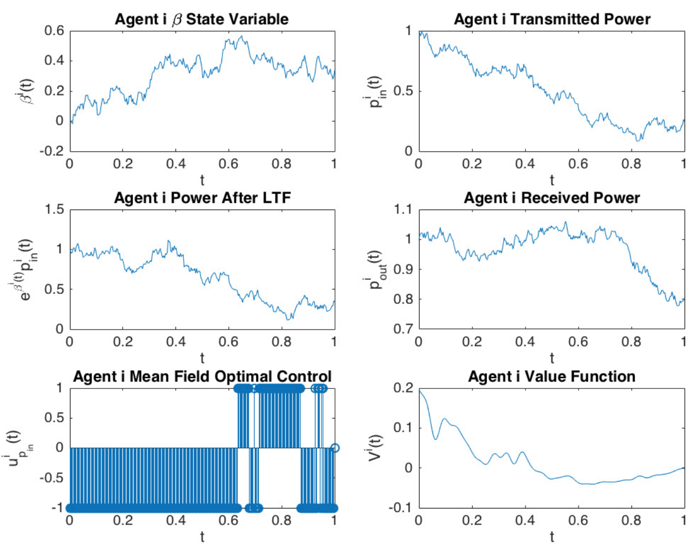


**Fig. 4.6** Sample path simulation of a generic agent's state, value function and controls

## 4.4 Simulation Results of the System With Agent Motion

As in the case of the CDMA problem without agent motion, we consider simulations of both the MFG PDE solution and particular random sample path behaviour of a particular generic agent. The dynamic SDE parameters are set to be $a = 0.1$, $b = 0.1$, $\sigma_\beta = \sigma_{p_{in}} = \sigma_{p_{out}} = 1$, $\nu = 0.1$, $\sigma_{x_1} = \sigma_{x_2} = 0.1$ and the noise power is chosen to be $\eta = 0.25$. The slow-fast parameter $\epsilon$ is given by $\epsilon = 0.01$. For the relevant discretization parameters, the final time is chosen to be $T = 1$ with $\Delta t = 0.005$. The domain is bounded by $\beta \in (\beta^{min}, \beta^{max}) = (-1, 1)$, $p_{in} \in (p_{in}^{min}, p_{in}^{max}) = (0, 3)$, $p_r \in (p_{out}^{min}, p_{out}^{max}) = (0, 6)$, $x_1 \in (x_1^{min}, x_1^{max}) = (-1.8, 1.8)$, and $x_2 \in (x_2^{min}, x_2^{max}) = (-1.8, 1.8)$. Also, it is set that $\Delta\beta = 0.2$, $\Delta p_{in} = 0.3$, $\Delta p_{out} = 0.6$ and $\Delta x_1 = \Delta x_2 = 0.18$. The system is further modelled as having the base station located at the origin $x_b = 0$. The initial Mean Field density $f_{\mu_0}$ is chosen to be a discretized approximation of the Gaussian distribution

$$\mathcal{N}\left(\begin{pmatrix} 0 \\ 1.5 \\ 3 \\ 0 \\ 0 \end{pmatrix}, \begin{pmatrix} 0.4 & 0 & 0 & 0 & 0 \\ 0 & 0.6 & 0 & 0 & 0 \\ 0 & 0 & 0.6 & 0 & 0 \\ 0 & 0 & 0 & 0.4 & 0 \\ 0 & 0 & 0 & 0 & 0.4 \end{pmatrix}\right).$$

As in Section 4.3, we first consider the results of applying Algorithm 1 with stopping condition $\epsilon_c = 0.001$ to solve the relevant MFG PDEs. The results are highlighted by presenting the dynamics of the joint marginal Mean Field density of the geometric state parameters $x_1$ and $x_2$, $f_{\mu_t}^{x_1,x_2}(x_1, x_2)$. The dynamics of this marginal density are shown in Fig. 4.7 where the density is shown for the particular times $t \in \{0, 0.5, 0.75, 1\}$.

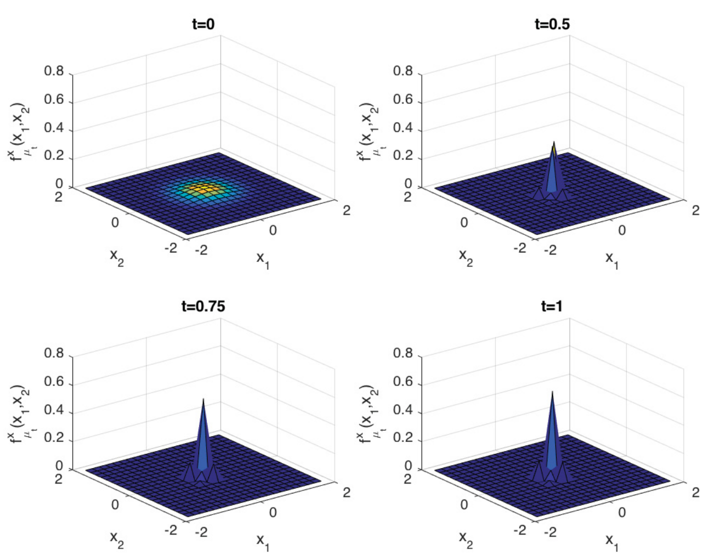


**Fig. 4.7** Dynamics of the marginal Mean Field density of $x$

The "marginal" value function of the generic agent with respect to the geometric variables $V_{x_1,x_2}(t,x_1,x_2)$ has corresponding dynamics shown in Fig. 4.8 where the value function is shown for times $t \in \{0, 0.5, 0.75, 1\}$.

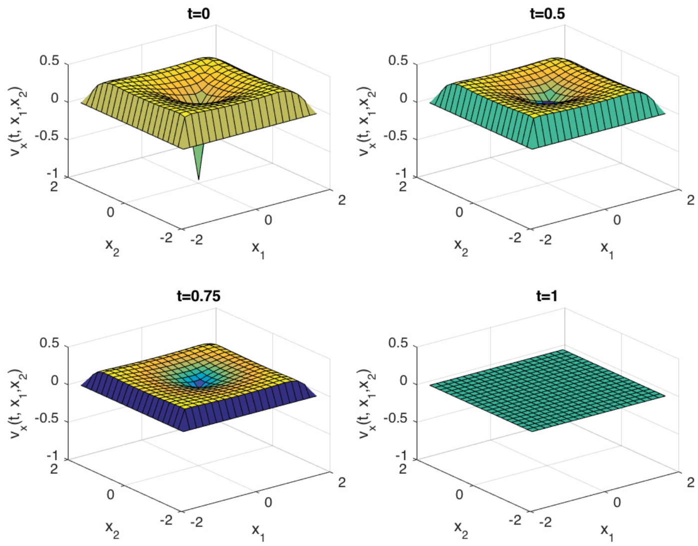


**Fig. 4.8** Dynamics of the value function of $x$

A notable observation is that the generic agent is moving in distribution to be closer to the base station. One can see that the density is somewhat approaching a point mass centred at the origin. The value function is consistent with this as it shows that agents have minimum costs near the origin. Therefore, movement towards the origin is in fact anticipated.

Fig. 4.9 depicts a sample path of an agent's geometric state variables as output from Algorithm 2 where the dynamic parameters are as before and the initial conditions are taken to be $(x_1)_0 = (x_2)_0 = 1$. As can be seen from both agent controls as well as state variable dynamics, the agents are trying to push their geometric variables to the origin.

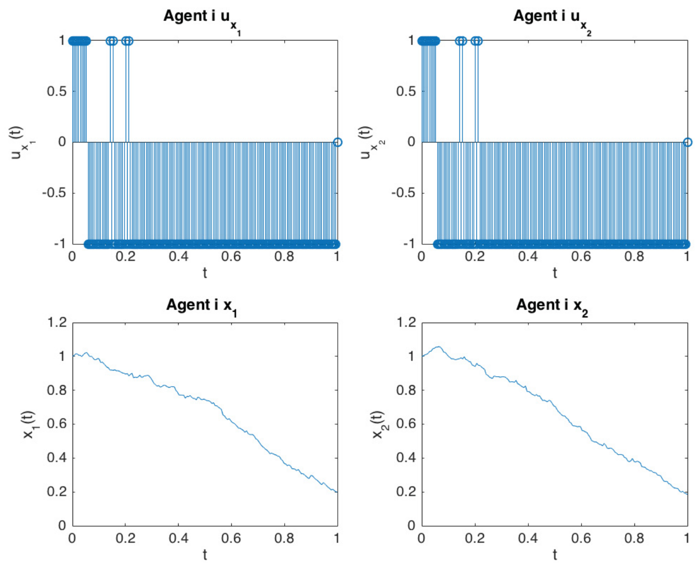


**Fig. 4.9** Individual sample paths of $x$ coordinates and their controls

Fig. 4.10 shows a two dimensional position plot of a particular generic agent's sample path in time with initial conditions $(x_1)_0 = (x_2)_0 = 1$ and dynamical parameters as before. The plot shows that in two dimensional space the agent is moving towards the origin with some random disturbances.

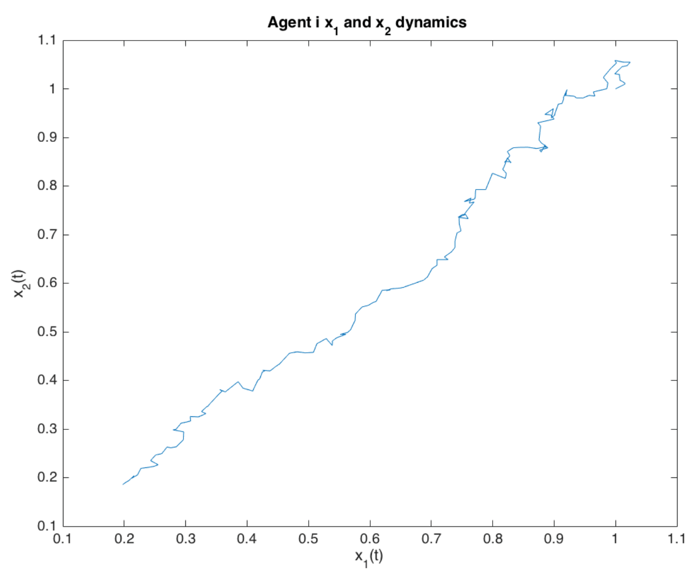


**Fig. 4.10** Position sample path of a generic agent

The two-dimensional plot of agent positions depicted by circles shown in Fig. 4.11 describes a system with 100 agents whose initial states are sampled according to the initial Mean Field density $f_{\mu_0}$. The agents use the infinite population MFG optimal controls as determined by Algorithm 1 in order to make decisions in time. The result shown in the simulation is that the agents are all crowding towards the base station as time varies from $t = 0$ to $t = 1$ which is consistent with the other results.

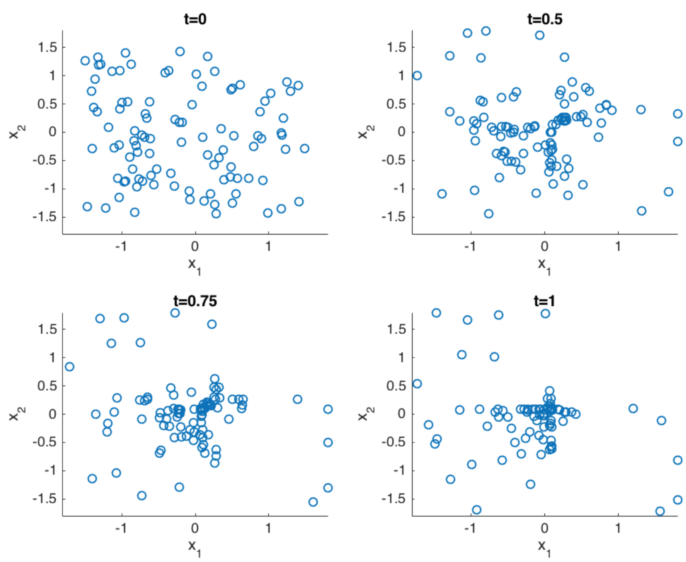


**Fig. 4.11** Two-dimensional plot of agent positions

## 4.5 Run Time and Memory Usage Comparison of the Problems

Following the approach in [17, 18] we now present run time and memory usage data of the execution of the numerical Algorithms for the MFG Loop of each of the non-localized and localized problem simulations in Section 4.3 and 4.4 respectively. The simulations were run on a 2.9 GHz Intel(R) Core(TM) i5 processor with 8 GB of 1867 MHz DDR3 RAM on a 64-bit operating system. Table 4.1 shows the resulting simulation data.

**Table 4.1** Numerical simulation performance data

| Problem | Dim. | Step Sizes | $\epsilon_c$ | Num. Iterations | Run Time (sec) | Memory (KB) |
|---|---|---|---|---|---|---|
| Non-Loc. | 4 | $\Delta_t = 0.003$, $\Delta_\beta = 0.1$, $\Delta_{p_{in}} = 0.15$, $\Delta_{p_{out}} = 0.3$ | $10^{-4}$ | 4 | 20.6 | 2350 |
| Non-Loc. | 4 | $\Delta_t = 0.003$, $\Delta_\beta = 0.1$, $\Delta_{p_{in}} = 0.15$, $\Delta_{p_{out}} = 0.3$ | $10^{-5}$ | 5 | 25.6 | 2350 |
| Localized | 6 | $\Delta_t = 0.003$, $\Delta_\beta = 0.1$, $\Delta_{p_{in}} = 0.15$, $\Delta_{p_{out}} = 0.3$, $\Delta_{x_1} = \Delta_{x_2} = 0.18$ | $10^{-3}$ | 3 | 2525.7 | 97459 |
| Localized | 6 | $\Delta_t = 0.003$, $\Delta_\beta = 0.1$, $\Delta_{p_{in}} = 0.15$, $\Delta_{p_{out}} = 0.3$, $\Delta_{x_1} = \Delta_{x_2} = 0.18$ | $10^{-4}$ | 5 | 4315.4 | 97459 |

The data shows that the increase in dimension (by 2) of the problem when adding agent motion increases the run time by an order of magnitude of 2 with the same stopping condition $\epsilon_c = 10^{-4}$.

An especially desirable feature of the Mean Field algorithms used in this work is that a large part of the solution can be precomputed off line and consequently it is important to highlight that the run times presented in the above table basically correspond to run times of an off line solution. This is important in a practical setting because in contemporary networks it is highly desired and often required that the on line time complexity of the power control algorithm applied is small.

# Chapter 5

# Decentralized Stochastic Control of OFDMA Femtocell Systems

## 5.1 Introduction

We consider an OFDMA femtocell downlink power control problem where the femtocell agents are transmitting data to each of their users over the different OFDMA frequency bands. The agents also take account for the behaviour of macrocell which in this case is modelled to be known ahead of time. The system is modelled as a competitive game with $N$ different agents or decision makers corresponding to the femtocells transmitting. Through the control of their transmit power over each band, agents are competing with each other in order to minimize their running cost (in time), specified by a linear combination of their quality of service (QoS) and transmit power.

## 5.2 Problem Formulation

We assume a femtocell network of $N$ agents using OFDMA communication. The system evolves in continuous time $t \in [0, T]$ and has finite horizon $T$, $0 < T < \infty$. There is a set of femtocell agents $A_i$, $1 \leq i \leq N$. There is also a set $R_j$, $1 \leq j \leq M$

of frequency resource blocks.

It is assumed that user association is fixed, i.e. that user devices are associated to a particular base station. Further it is assumed that resource block association is fixed, i.e. that the different frequency blocks are already allocated to corresponding user devices for the time period considered. It is also assumed that the dynamic state of the macrocell, namely its transmit power and channel attenuation, is known ahead of time by the femtocell agents. This model considers power control over one time period $[0, T]$ of the downlink transmission of each base station in a femtocell network over each resource block as a decentralized dynamic game.

In addition to the state variables to be discussed in the Section 5.3, it is assumed that each agent $i$ has a state variable $x_i \in \mathbb{R}^2$ corresponding to the (static) position in two dimensional space of the femtocell. This state variable is considered to be the *type* of the agent. It is also assumed that the macrocell is located at the origin and that the femtocells are spread out in space according to the probability density function $f_{x_1,x_2}(x_1, x_2)$ and that this density function is known to all agents and is the only information each agent has about the other agents' locations (types).

## 5.3 Agent State Variables and Dynamics

As in Chapter 3, the problem models agent states as containing the information of both channel attenuation and transmit power over each of the frequency bands. The log-normal generalized SDE model is used as a channel model for this problem. The state of agent $A_i$, $0 \leq i \leq N$, is given by the two state (vector) dynamic variables $\beta_i(t) \in \mathbb{R}^M$ and $p_i(t) \in \mathbb{R}_+^M$ corresponding to the vectors of attenuation parameters over each frequency block and the transmit power over each frequency block of the given agent respectively. The attenuation vector variable $\beta_i(t)$ is defined as

$$\beta_i(t) = \begin{pmatrix} \beta_i^1(t) \\ \vdots \\ \beta_i^M(t) \end{pmatrix} \tag{5.1}$$

where each $\beta_i^j(t)$, $1 \leq j \leq M$ corresponds to the attenuation parameter of transmission over resource block $R_j$. For each attenuation parameter $\beta_i^j(t)$, the dynamics follow the following uncontrolled stochastic differential equation

$$d\beta_i^j(t) = -a_i(\beta_i^j(t) + b_i)dt + \sigma_{\beta_i}^2 dW_{\beta_i^j}(t), \quad \beta_i^j(0) = (\beta_i^j)_0 \tag{5.2}$$

where $a_i > 0$, $b_i > 0$, $\sigma_{\beta_i} > 0$ for all $i$, $1 \leq i \leq N$ and $W_{\beta_i^j}(t) \in \mathbb{R}$ is a standard Wiener process independent of all other mutually independent Wiener processes and initial conditions $(\beta_i^j)_0$.

The transmit power vector $p_i(t)$ is defined by

$$p_i(t) = \begin{pmatrix} p_i^1(t) \\ \vdots \\ p_i^M(t) \end{pmatrix} \tag{5.3}$$

which correspond to the transmit power over each resource block. For each power variable, the dynamics follow the following SDE

$$dp_i^j(t) = u_i^j(t)dt + \sigma_{p_i}^2 dW_{p_i^j}(t), \quad p_i^j(0) = (p_i^j)_0 \tag{5.4}$$

where $\sigma_{p_i} > 0$, $u_i^j(t) \in [-1, 1]$ and $W_{p_i^j}(t) \in \mathbb{R}$ is a standard Wiener process independent of all other mutually independent Wiener processes and initial conditions $(p_i^j)_0$. The output power of the particular channel $j$, $1 \leq j \leq M$, corresponding to the transmitted signal of agent $i$ to its corresponding user device is given by $e^{\beta_i^j(t)} p_i^j(t)$

for all $1 \leq i \leq N$.

In this model, the parameters of the dynamical equations of both the power and attenuation processes are independent of frequency resource, i.e. the SDEs governing the agent states have identical parameters over each resource block (and hence do not depend on $j$). For all $i : 1 \leq i \leq N$, the dynamics are uniform, i.e. $a_i = a$, $b_i = b$, $\sigma_{\beta_i} = \sigma_\beta$, $\sigma_{p_i} = \sigma_p$.

## 5.4 Agent Cost Functions

Agent costs are modelled as a linear combination of signal-to-interference-plus-noise-ratio (SINR) and transmit power. Before explicitly providing an expression for SINR (and corresponding cost functions) it is first noted that the distance between a femtocell and its corresponding user is assumed to be negligible compared to the distance between femtocells. Further, since the problem is considered in the downlink and that interference occurs at the user devices, in order to compute path loss, one needs to know the distance between each femtocell and each corresponding user device. It is therefore assumed that the distance between a given user device and an interfering femtocell base station is approximately equal to the distance between that interfering base station and the femtocell base station to which the user device is associated. More explicitly, at time $t$, user device $j$ (associated to frequency resource $j$), $1 \leq j \leq M$ of femtocell agent $i$, $1 \leq i \leq N$ experiences an interfering signal from agent $k$, $1 \leq k \leq N$, $k \neq i$ with power $e^{-||x_i - x_k||^2} e^{\beta_k^j(t)} p_k^j(t)$ where $|| \cdot ||$ denotes the Euclidean norm in $\mathbb{R}^2$. It is remarked that the path loss exponent $-||x_i - x_k||^2$ uses the distance between femtocell agent $i$ and femtocell agent $k$ and does not explicitly use the position of the user device which is abstracted from the problem.

An expression for the SINR is now formulated. The SINR of agent $A_i$, $1 \leq i \leq N$, over frequency resource $R_j$, $1 \leq j \leq M$, is given by

$$\gamma_i^j(t) = \frac{e^{\beta_i^j(t)} p_i^j(t)}{\sum_{k=1,k\neq i}^{N} e^{-||x_i - x_k||^2} e^{\beta_k^j(t)} p_k^j(t) + e^{-||x_i||^2} e^{\beta_m^j(t)} p_m^j(t) + \eta} \tag{5.5}$$

where all variables are defined as previously, $\beta_m^j(t) \in \mathbb{R}$ and $p_m^j(t) \in \mathbb{R}_+$ correspond to the known attenuation parameter and transmit power of the macrocell over frequency resource $R_j$ and $\eta$ is the thermal noise in the channel. It is remarked that the SINR expression is considered as a per-frequency-resource quantity. This is due to the fact that in OFDMA communication, signals transmitted over different frequency resources do not interfere due to the orthogonality of the frequency resources.

Two models are provided for the loss function of each agent $i$, $1 \leq i \leq N$. The first considers the case where each of the agents is aiming to maximize social well fare (over time) by minimizing the time integrated loss of the sum of costs over each of its user devices, which in this formulation, corresponds to the sum of costs over each transmitting resource block. The corresponding instantaneous loss function is defined as

$$L_i(t, u_i, u_{-i}) = \sum_{j=1}^{M} \left( -\gamma_i^j(t) + \frac{1}{N} p_i^j(t) \right) \tag{5.6}$$

where here, the coefficient $\frac{1}{N}$ is a normalization coefficient introduced with the purpose of keeping the two cost metrics (QoS and transmit power) of the same orders of magnitude of $N$.

The second case of loss function considered is that of each agent playing an independent game with other agents over each of the different frequency slots. Therefore, for each dynamic game, the per resource consider per resource block costs (thus dividing the system into $M$ different games)

$$L_i^j(t, u_i, u_{-i}) = -\gamma_i^j(t) + \frac{1}{N} p_i^j(t) \tag{5.7}$$

where the coefficient $\frac{1}{N}$ is again introduced for reasons identical to those in (5.6).

In this case of this loss function, the original dynamic game is played instead as $M$ independent games where in each game $j$ (one for each frequency resource $j$), $1 \le j \le M$, agent $i$, $1 \le i \le N$ has only two dynamic state variables $\beta_i^j(t) \in \mathbb{R}$ and $p_i^j(t) \in \mathbb{R}_+$. For reasons of computational efficiency, the second case of costs will be considered for the remainder of the work. Due to the independent games being played over each frequency slot, the subscript $j$ is dropped in the majority of the analysis for the purpose of brevity. The cost-to-go of a given agent $A_i$ is given by

$$J_i^N(s,u_i, u_{-i}, \tilde{\theta}_i; x_i) \triangleq E\left[\int_s^T L_i^N(t, u_i, u_{-i})dt \middle| \theta_i(s) = \tilde{\theta}_i\right] \tag{5.8}$$

$$= E\Big[\int_s^T \Big( - \frac{e^{\beta_i(t)}p_i(t)}{\sum_{k=1,k\neq i}^N e^{-||x_i - x_k||^2} e^{\beta_k(t)}p_k(t) + e^{-||x_i||^2}e^{\beta_m(t)}p_m(t) + \eta} + \frac{1}{N}p_i(t)\Big)dt \Big| \theta_i(s) = \tilde{\theta}_i\Big] \tag{5.9}$$

where $\theta_i(t) = \begin{pmatrix} \beta_i(t) \\ p_i(t) \end{pmatrix}$ and we explicitly note the parametrization of the cost by the static position $x_i$ of agent $i$.

## 5.5 Mean Field Games Analysis

The steps involved in applying Mean Field Game (MFG) theory in this chapter and the computational methods used very closely follow the general steps in Chapters 3 and 4. We note that for conciseness, certain details are omitted in the discussion in this chapter when they may be assumed to be followed in a straightforward manner from the detailed counterparts presented in Chapters 3 and 4.

### 5.5.1 Middle Population Argument and Generic Agent State Extension

Unfortunately, one cannot apply a standard MFG analysis to the system (5.2), (5.4), (5.9) by taking the infinite population limit due to the divergence of the sum in the denominator of the agent cost function (5.9) as $N \to \infty$. Instead, a middle population argument is applied which is assumed to be valid for $N$ of moderate size; for the problem under consideration this is considered to mean that $N$ is on the order of magnitude of $50 \leq N \leq 100$ corresponding to a typical real life single macrocell femtocell network.

In the middle population range, the generic agent cost function is constructed using (i) an infinite population average interference given by a Mean Field integral and (ii) an approximation error process which models the difference between the actual average interference and the Mean Field integral. As a result, the generic agent cost functions do not assume an infinite population system but rather include an infinite population limiting average as an approximation while also taking account of the approximation error involved with respect to the population of middle sized $N$. This is in contrast to the standard MFG approach where the generic agent cost functions use only an infinite population limiting average as an approximation to the large population behaviour. Each of the middle population approximations and assumptions are now described in detail.

#### Generic Agent Dynamics

Because the dynamics of each agent are the same, irrespective of the size of the population $N$, we let the dynamics of the generic agent be identical to the dynamics of each agent prior to the system approximation given by the SDEs in (5.2) and (5.4). We recall that in the separated game (i.e. that where the frequency blocks are considered separately) the agent processes $\beta_i(t)$ and $p_i(t)$ are one dimensional.

### Generic Agent Costs Using Middle Population Approximation

The cost-to-go of the generic agent in the middle population range is given by (5.10).

$$J_i^{mid}(s, u_i, u_{-i}, \tilde{\theta}_i; x_i) = E\left[\int_s^T L_i^{mid}(t, u_i, u_{-i})dt \middle| \theta_i(s) = \tilde{\theta}_i\right] \tag{5.10}$$

and correspondingly the middle population loss function of generic agent $i$ is given by

$$L_i^{mid}(t, u_i, u_{-i}) = -\frac{e^{\beta_i(t)}p_i(t)}{NI(t) + z_i(t) + e^{-||x_i||^2}e^{\beta_m(t)}p_m(t) + \eta} + \frac{1}{N}p_i(t) \tag{5.11}$$

where $z_i(t)$ is to be defined, and $I(t)$ is the Mean Field integral term given by

$$I(t) = \lim_{N\to\infty} \frac{1}{N} \sum_{k=1,k\neq i}^{N} e^{-||x_i - x_k||^2} e^{\beta_k(t)} p_k(t) \tag{5.12}$$

$$= \int_{\Omega_\theta \times \Omega_x} e^{-||x_i - x||^2} e^{\beta} p f_{\mu_t}(\theta|x) f_x(x) dx d\theta \tag{5.13}$$

Here $\theta = \begin{pmatrix}\beta & p & z\end{pmatrix}^T$, $f_{\mu_t}(\theta|x) = f_{\mu_t}(\beta, p, z|x_1, x_2)$ is the conditional probability density function, conditioned on the location (type), of the Mean Field at time $t \in [0, T]$, $\Omega_\theta = \Omega_\beta \times \Omega_p \times \Omega_z$ is the support set of $f_{\mu_t}$ and $f_x(x) = f_{x_1,x_2}(x_1, x_2)$, and $z$ is an argument of $f_{\mu_t}$ corresponding to a new state variable which is to be defined. Here, we have made the following assumption

> (**M1**) There exists a Mean Field measure $\mu_t$ with corresponding density $f_{\mu_t}$ such that the limit of the average interference power given by (5.12), as the number of agents $N$ goes to infinity, converges to the Mean Field integral (5.13).

The variable $z_i(t) \in \mathbb{R}$ in (5.11) then corresponds to the approximation error incurred by modelling the actual average interference power by the Mean Field integral expression. More explicitly,

$$z_i(t) = \frac{1}{N}\sum_{k=1,k\neq i}^{N} e^{-||x_i-x_k||^2} e^{\beta_k(t)} p_k(t) - \int_{\Omega_\theta\times\Omega_x} e^{-||x_i-x||^2} e^{\beta} p f_{\mu_t}(\theta|x) f_x(x) dx d\theta \tag{5.14}$$

We shall make the following second assumption

> (**M2**) The approximation error $z_i(t)$ is a random process which is independent of all other random processes and variables in the loss function (5.11) including $\beta_i(t)$ and $p_i(t)$ as well as the macrocell states $\beta_m(t)$ and $p_m(t)$ and the channel noise $\eta$.

### Generic Agent State Extension

We now make the third assumption

> (**M3**) The dynamics of approximation error process $z_i(t)$ in the generic agent loss function (5.11) are given by an SDE and the state vector of the generic agent is extended to include $z_i(t)$.

Naturally, given the assumed state extension, the Mean Field measure (and corresponding density $f_{\mu_t}$) now carry the joint statistical information of this process with the other state variables.

In this work in particular, the following linear SDE for a uniformly parametrized population is used to approximate the dynamics of the approximation error:

$$dz_i(t) = -\alpha z_i(t)dt + \sigma_z dW_{z_i}(t), \qquad z_i(0) = (z_i)_0 \tag{5.15}$$

where $\alpha >> 0$ and $\sigma_z > 0$ and $W_{z_i}(t)$ is a standard Wiener process.

#### Generic Agent Value Function

The value function of the generic agent $i$, again parametrized by the position $x_i$ of agent $i$ is then defined as

$$V_i(s, \tilde{\theta}_i; x_i) = \inf_{u \in U} J_i^{mid}(s, u, \tilde{\theta}_i; x_i) \tag{5.16}$$

### 5.5.2 MFG Equations and Nonlinear Loop

In this problem, there is a loop relation between the conditional Mean Field density $f_{\mu_t}(\beta, p, z|x_1, x_2)$, the position parametrized value function $V(t, \beta, p, z; x_1, x_2)$ and the best response controls of the generic agent (also parametrized by its position), $u^*(t, \beta, p, z; x_1, x_2)$. The loop relation exists through the coupling of the MFG equations which are defined in this section. It is assumed that all conditions are met for a nonlinear contraction principle on the MFG Loop. For the MFG PDEs in the following analysis we assume a state domain of $D$, i.e. $\theta \in D$.

#### The MFG HJB Equation and Best Response Controls

We begin with the MFG HJB equation of the generic agent which given the conditional Mean Field density, $f_{\mu_t}(\beta, p, z|x_1, x_2)$ describes the evolution of the parametrized value function $V(t, \beta, p, z; x_1, x_2)$. The equation is given below.

$$\begin{aligned} -\frac{\partial V}{\partial t} &= \frac{\sigma_\beta^2}{2}\frac{\partial^2 V}{\partial \beta^2} + \frac{\sigma_p^2}{2}\frac{\partial^2 V}{\partial p^2} + \frac{\sigma_z^2}{2}\frac{\partial^2 V}{\partial z^2} - a(\beta + b)\frac{\partial V}{\partial \beta} - \alpha z \frac{\partial V}{\partial z} + \frac{1}{N}p \\ &- \frac{e^\beta p}{N \int_{\Omega_\theta \times \Omega_{\overline{x}}} e^{-||x - \overline{x}||^2} e^\beta p f_{\mu_t}(\theta|\overline{x}) f_x(\overline{x}) d\overline{x} d\theta + e^{-||x||^2} e^{\beta_m(t)} p_m(t) + z + \eta} \\ &+ \inf_{u \in U}\left\{u \frac{\partial V}{\partial p}\right\}, \quad V(T, \theta) = 0, \quad (t, \theta) \in [0, T] \times D \end{aligned} \tag{5.17}$$

The best response is given by the minimization of the Hamiltonian in the MFG HJB and has solution

$$u^*(t, \beta, p, z; x_1, x_2) = -sign\left\{\frac{\partial V}{\partial p}\right\} \tag{5.18}$$

### The MFG FPK Equation

The MFG FPK equation given the best response control $u^*(t, \beta, p, z; x_1, x_2)$ and describing the dynamics of the conditional Mean Field density $f_{\mu_t}(\beta, p, z|x_1, x_2)$ is given below

$$\begin{aligned}\frac{\partial f_{\mu_t}}{\partial t} &= -\frac{\partial}{\partial \beta}[-a(\beta+b)f_{\mu_t}] - \frac{\partial}{\partial p}[uf_{\mu_t}] - \frac{\partial}{\partial z}[-\alpha z f_{\mu_t}] \\ &+ \frac{1}{2}\frac{\partial^2}{\partial \beta^2}[\sigma_\beta^2 f_{\mu_t}] + \frac{1}{2}\frac{\partial^2}{\partial p^2}[\sigma_p^2 f_{\mu_t}] + \frac{1}{2}\frac{\partial^2}{\partial z^2}[\sigma_z^2 f_{\mu_t}], \qquad (t,\theta) \in [0,T] \times D\end{aligned} \tag{5.19}$$

## 5.6 Computational Investigations and Simulations

Computation is now used in order to solve numerically for both the solutions of the MFG PDEs and particular sample paths of a generic agent. We apply numerical algorithms almost identical to Algorithms 1 and 2 of Chapter 4 with the dynamics and costs relevant to this problem.

The parameters are chosen to be $N = 50$, $a = 0.5$, $b = 0.5$, $\sigma_\beta = 0.2$, $\sigma_p = 0.4$, $\alpha = 1$, $\sigma_z = 1$ and $\eta = 0.25$. For the relevant discretization parameters, the final time is set as $T = 1$ with $\Delta t = \frac{1}{200}$. The domain is bounded by $\beta \in (-1, 1)$, $p \in (0, 3)$, $z \in (-1, 1)$ and $x_1, x_2 \in (-1, 1)$. Also it is set that $\Delta\beta = 0.1$, $\Delta p = 0.15$, $\Delta z = \Delta x_1 = \Delta x_2 = 0.2$. The probability density function $f_{x_1,x_2}(x_1, x_2)$ of agent types is chosen to be given by a discretized approximation of the Gaussian distribution $\mathcal{N}\left(\begin{pmatrix}0\\0\end{pmatrix}, \begin{pmatrix}0.4 & 0\\ 0 & 0.4\end{pmatrix}\right)$. The initial conditional Mean Field density $f_{\mu_t}(\beta, p, z|x_1, x_2)$ is chosen to be given by a discretized approximation of the Gaussian distribution $\mathcal{N}\left(\begin{pmatrix}0.5\\1.25\\0\end{pmatrix}, \begin{pmatrix}0.4 & 0 & 0\\ 0 & 0.6 & 0\\ 0 & 0 & 0.4\end{pmatrix}\right)$ independent of agent type. The macrocell states $\beta_m(t)$ and $p_m(t)$ are chosen to be driven by simple standard Wiener processes with initial conditions $\beta_m(0) = 0$ and $p_m(0) = 10$.

A simulation of Algorithm 1 is first investigated where the MFG Loop is solved.

The stopping condition is set to be $\epsilon_c = 0.001$. Fig. 5.1 shows the resulting joint marginal Mean Field density of state parameters $\beta$ and $p$ defined as

$$f_{\mu_t}^{\beta,p}(\beta, p) = \int_{\Omega_z \times \Omega_x} f_{\mu_t}(\beta, p, z|x) f_x(x) dz dx \tag{5.20}$$

at the times $t \in \{0, 0.5, 0.75, 1\}$.

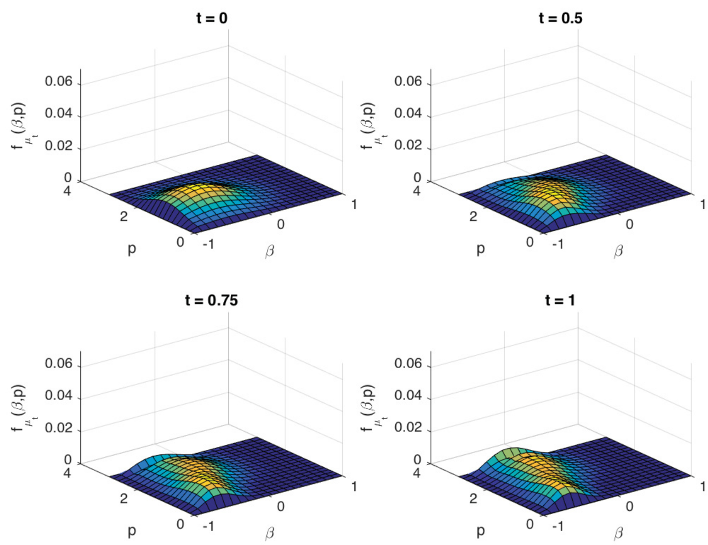


**Fig. 5.1** Dynamics of the marginal Mean Field density of $\beta$ and $p$

The dynamics of the corresponding "marginal" value function of the generic agent of state parameters $\beta$ and $p$ denoted as $V_{\beta,p}(t, \beta, p)$ which is defined to be

$$V_{\beta,p}(t, \beta, p) = \int_{\Omega_z \times \Omega_x} V(t, \beta, p, z; x) f_{\mu_t}(\beta, p, z|x) f_x(x) dz dx \tag{5.21}$$

are shown in Fig. 5.2.

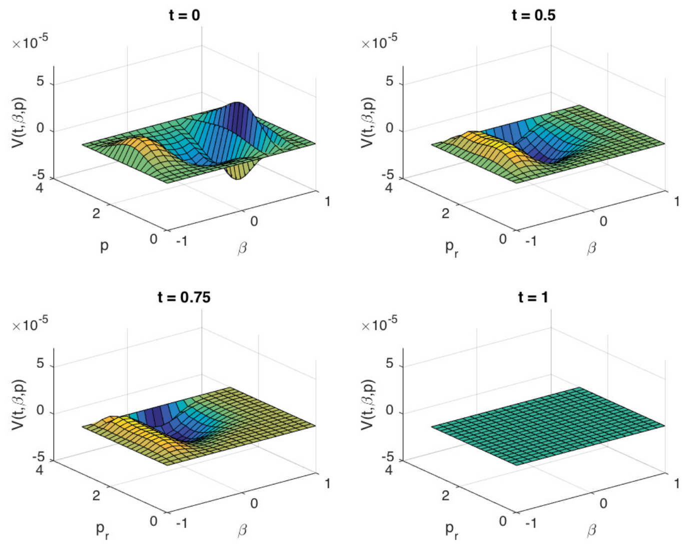


**Fig. 5.2** Dynamics of the value function of $\beta$ and $p$

Finally, we present results of simulations conducted using Algorithm 2 in order to compute a sample path of a generic agent state. All SDE parameters are set as before and the initial conditions are chosen to be $\beta_0 = -0.5$, $p_0 = 1.25$ and $z_0 = 0$ for an agent located at $x_1 = x_2 = 0.5$. Fig. 5.3 shows the results of the simulation.

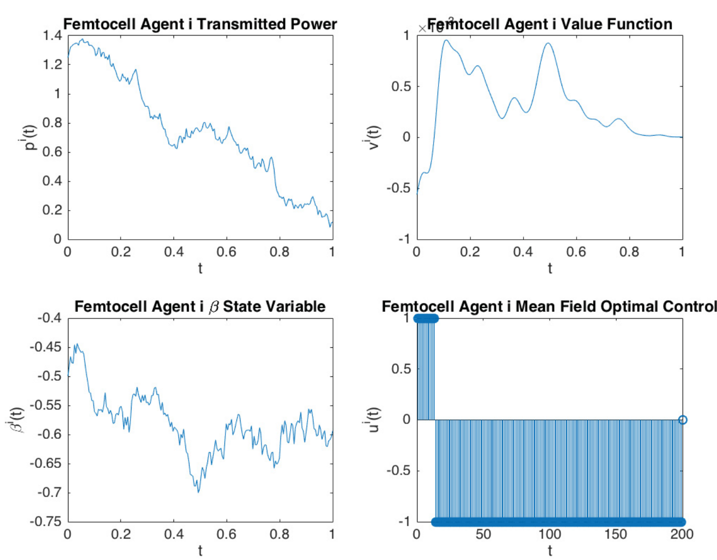


**Fig. 5.3** Sample path simulations of a generic agent

# Chapter 6

# Conclusion and Future Research

## 6.1 Conclusion

In this thesis we investigate decentralized power control in cellphone networks using channel modelling and Mean Field Game theory.

First, a new continuous time state-space nonlinear channel model is developed which combines the effects of long-term and short-term fading into a compact combined model. Through analysis and illustrative simulations, it is shown that the model follows traditional wireless channel modelling principles while also offering additional continuous-time dynamic information.

Second, two CDMA cellphone network optimization problems are formulated using the new channel model; these problems are then solved through an analysis of the resulting MFG equations and the utilization of relatively simple numerical algorithms. Extensive illustrative simulations are then provided.

In the last part of the thesis we investigate the continuous-time state space modelling of OFDMA femtocell systems and then formulate a decentralized power control problem where the femtocells are competing against each other in order to provide acceptable QoS to their user devices while also maintaining transmit power efficiency. A solution to this OFDMA power control problem is then provided in the thesis by an application of MFG theory and what has been termed middle population approximations, together with straightforward numerical algorithms.

## 6.2 Future Research

This work has immediate extensions. First, extensions of the CDMA optimization problems considered can be developed using the extended channel model introduced in Section 2.6 involving Poisson jumps which more accurately account for rapid changes in long-term fading gains due to the presence of large obstacles. In order to do this, some extensions of MFG theory would have to be investigated and applied.

Second, it would be of interest to carry out analytic and numerical comparisons of the performance of the MFG CDMA decentralized network control algorithms presented in this thesis with centralized control algorithms formulated, for instance, in terms of Mean Field Type Control theory [41].

Third, the work has considered an application of MFG theory to OFDMA femtocell systems in the particular case of the power control over one time slot of OFDMA communication. In effect, an extension of this work would be to consider combinatorial methods in order to solve for the problem of allocating different frequency resources to the various cellphone user devices at each time slot at the high level while applying the used MFG methodology for the power control over each of these frequency resources during each time slot at the low level.

Fourth, the cellphone game problems in Chapters 3, 4 and 5 are modelled and analysed in continuous time and the applied Mean Field control algorithms are implicitly solving a discrete time model via state and PDE discretization. It could therefore be of interest to extend the models and results of the work to discrete time.

Finally, Chapter 5 introduces new theoretical considerations for MFG theory; this work results in ideas for the further exploration of applications of MFG theory to middle population systems where one cannot directly apply traditional infinite population approximations without also considering non-negligible approximation errors. The simulations completed are encouraging and provide meaningful results but theoretical extensions of the MFG framework would be required to analytically discuss these results. In effect, further theoretical explorations might in fact lead to an extension to the MFG framework which takes account for middle population systems such as the OFDMA femtocell system considered in this work.

# Appendix A

# Probability Density Functions

### Log-normal Random Variables

The probability density function of a log-normal random variable is given by

$$f(x) = \frac{1}{x\sigma\sqrt{2\pi}} \exp\left(\frac{-(\ln x - \mu)^2}{2\sigma^2}\right), x > 0, \mu \in \mathbb{R}, \sigma \in \mathbb{R}_+ \tag{A.1}$$

where $\sigma^2$ and $\mu$ are the log variance and log mean.

### Rayleigh Random Variables

The probability density function of a Rayleigh random variable is given by

$$f(r) = \frac{r}{\sigma^2} \exp\left(-\frac{r^2}{2\sigma^2}\right), r \geq 0, \sigma \in \mathbb{R}_+ \tag{A.2}$$

### Rician Random Variables

The probability density function of a Rician random variable is given by

$$f(r) = \frac{r}{\sigma^2} \exp\left(-\frac{r^2 + \nu^2}{2\sigma^2}\right) I_0(r\nu/\sigma^2), r \geq 0, \nu, \sigma \in \mathbb{R}_+ \tag{A.3}$$

where $I_0(\cdot)$ is the modified Bessel function of the first kind of order zero given by

$$I_0(x) = \sum_{m=0}^{\infty} \frac{1}{(m!)^2} \left(\frac{x}{2}\right)^{2m} \tag{A.4}$$

# Appendix B

# Sobolev Spaces and Weak Derivatives

The following are definitions of of weak derivatives and Sobolev spaces as defined in Chapter 5 of [38].

## B.1 Weak Derivatives

**Notation 1.** *Let $C_c^\infty(U)$ denote the space of infinitely differentiable functions $\phi : U \to \mathbb{R}$, with compact support in $U$. A function $\phi$ belonging to $C_c^\infty(U)$ is called a test function.*

**Definition 1.** *Suppose $u, v \in L^1_{loc}(U)$, and $\alpha$ is a multiindex. It is said that $v$ is the $\alpha$-th weak partial derivative of $u$, written*

$$D^\alpha u = v, \tag{B.1}$$

*provided*

$$\int_U u D^\alpha \phi dx = (-1)^{|\alpha|} \int_U v \phi dx \tag{B.2}$$

*for all test functions $\phi \in C_c^\infty(U)$.*

## B.2 Sobolev Spaces

Let $1 \leq p \leq \infty$ and let $k$ be a nonnegative integer.

**Definition 2.** *The Sobolev space* $W^{k,p}(U)$ *consists of all locally summable functions* $u : U \to \mathbb{R}$ *such that for each multiindex* $\alpha$ *with* $|\alpha| \leq k$, $D^\alpha u$ *exists in the weak sense and belongs to* $L^p(U)$. *If* $p = 2$, *it is usually written* $H^k(U) = W^{k,2}(U)$ $(k = 0, 1, 2, ...)$.

**Definition 3.** $W_0^{k,p}(U)$ *denotes the closure of* $C_c^\infty(U)$ *in* $W^{k,p}(U)$. *It is customary to write* $H_0^k(U) = W_0^{k,2}(U)$.

**Definition 4.** $H^{-1}(U)$ *denotes the dual space to* $H_0^1(U)$. *In other words* $f$ *belongs to* $H^{-1}(U)$ *provided* $f$ *is a bounded linear functional on* $H_0^1(U)$.

# Appendix C

# Square Root Process Average Power

The following is a derivation of the long-term average value of a square-root process. Consider (S) below for $x_t \in \mathbb{R}$, $t \in \mathbb{R}_+$

$$(S): \qquad dx_t = \alpha(\gamma - x_t)dt + \sigma\sqrt{x_t}dw_t \tag{C.1}$$

where $\alpha, \gamma, \sigma > 0$ and $w_t$ is a standard Wiener process. Integrating (S) gives:

$$(S^I): \qquad (\gamma - x_T) - (\gamma - x_0) = -\alpha\int_0^T(\gamma - x_t)dt - \sigma\int_0^T\sqrt{x_t}dw_t \tag{C.2}$$

Taking expectations in $(S^I)$ yields:

$$(S^{IE}): \qquad \frac{E(\gamma - x_T)}{T} - \frac{E(\gamma - x_0)}{T} = \alpha E\left[\frac{1}{T}\int_0^T(x_t - \gamma)dt\right] \tag{C.3}$$

But the convolution solution to (S) is:

$$(x_T - \gamma) = e^{-\alpha T}(x_0 - \gamma) - \sigma\int_0^T e^{-\alpha(T-t)}\sqrt{x_t}dw_t \tag{C.4}$$

Hence

$$(E): \qquad \frac{E\tilde{x}_T}{T} = \frac{E(x_T - \gamma)}{T} = \frac{1}{T}Ee^{-\alpha T}(x_0 - \gamma) \tag{C.5}$$

Therefore,

$$\left|\frac{E\tilde{x}_T}{T}\right| \leq \frac{1}{T}E\left|e^{-\alpha T}(x_0 - \gamma)\right| \to 0 \text{ as } T \to \infty \tag{C.6}$$

So from $(S^{IE})$:

$$\begin{aligned}
\lim_{T\to\infty}\frac{1}{T}E\int_0^T \alpha x_t dt &= \lim_{T\to\infty}\frac{\alpha}{T}E\int_0^T \gamma dt + \lim_{T\to\infty}\frac{E(\gamma - x_T)}{T} - \lim_{T\to\infty}\frac{E(\gamma - x_0)}{T} && \text{(C.7)}\\
&= \alpha\gamma + \lim_{T\to\infty}\frac{1}{T}Ee^{-\alpha T}(x_0 - \gamma) && \text{(C.8)}\\
&= \alpha\gamma + \frac{1}{T}Ee^{-\alpha T}(x_0 - \gamma) \qquad \text{by (E)} && \text{(C.9)}\\
&= \alpha\gamma && \text{(C.10)}
\end{aligned}$$

Therefore,

$$\gamma = \lim_{T\to\infty}\frac{1}{T}E\int_0^T x_t dt \tag{C.11}$$

as required.

# References

[1] A. Goldsmith, *Wireless Communications.* New York, NY, USA: Cambridge University Press, 2005.

[2] H. S. Dhillon, R. K. Ganti, F. Baccelli, and J. G. Andrews, "Modeling and analysis of k-tier downlink heterogeneous cellular networks," *IEEE Journal on Selected Areas in Communications*, vol. 30, pp. 550–560, April 2012.

[3] National Instruments, "Introduction to lte device testing from theory to transmitter and receiver measurements."

[4] C. Charalambous and N. Menemenlis, "General non-stationary models for short-term and long-term fading channels," in *EUROCOMM 2000. Information Systems for Enhanced Public Safety and Security. IEEE/AFCEA*, pp. 142–149, 2000.

[5] D. Lopez-Perez, A. Valcarce, G. de la Roche, and J. Zhang, "Ofdma femtocells: A roadmap on interference avoidance," *IEEE Communications Magazine*, vol. 47, pp. 41–48, September 2009.

[6] E. Hossain, M. Rasti, H. Tabassum, and A. Abdelnasser, "Evolution toward 5g multi-tier cellular wireless networks: An interference management perspective," *IEEE Wireless Communications*, vol. 21, pp. 118–127, June 2014.

[7] C. E. Shannon, "Communication in the presence of noise," *Proc. Institute of Radio Engineers*, vol. 37, no. 1, pp. 10–21, 1949.

[8] D. Tse and P. Viswanath, *Fundamentals of Wireless Communication*. New York, NY, USA: Cambridge University Press, 2005.

[9] M. Huang, P. Caines, and R. Malhame, "Individual and mass behaviour in large population stochastic wireless power control problems: centralized and nash equilibrium solutions," in *Proceeding 42nd IEEE Conference on Decision and Control*, vol. 1, pp. 98–103 Vol.1, Dec 2003.

[10] M. Huang, R. P. Malhamé, and P. E. Caines, "Large population stochastic dynamic games: closed-loop mckean-vlasov systems and the nash certainty equivalence principle," *Communications in Information and Systems*, vol. 6, no. 3, pp. 221–252, 2006.

[11] M. Huang, P. Caines, and R. Malhame, "Large-population cost-coupled lqg problems with nonuniform agents: Individual-mass behavior and decentralized epsilon-nash equilibria," *IEEE Transactions on Automatic Control*, vol. 52, pp. 1560–1571, Sept 2007.

[12] J.-M. Lasry and P.-L. Lions, "Jeux à champ moyen. {I} le cas stationnaire," *Comptes Rendus Mathematique*, vol. 343, no. 9, pp. 619 – 625, 2006.

[13] J.-M. Lasry and P.-L. Lions, "Jeux à champ moyen. {II} horizon fini et contrôle optimal," *Comptes Rendus Mathematique*, vol. 343, no. 10, pp. 679 – 684, 2006.

[14] J.-M. Lasry and P.-L. Lions, "Mean field games," *Japanese Journal of Mathematics*, vol. 2, no. 1, pp. 229–260, 2007.

[15] P. Caines, "Mean field games," in *Encyclopedia of Systems and Control* (J. Baillieul and T. Samad, eds.), pp. 1–6, Springer London, 2014.

[16] M. Nourian and P. E. Caines, "$\epsilon$-nash mean field game theory for nonlinear stochastic dynamical systems with major and minor agents," *SIAM Journal on Control and Optimization*, vol. 51, no. 4, pp. 3302–3331, 2013.

[17] M. Aziz and P. Caines, "Computational investigations of decentralized cellular network optimization via mean field control," in *Proceeding 53rd IEEE Conference on Decision and Control*, pp. 5560–5567, Dec 2014.

[18] M. Aziz and P. Caines, "A mean field control computational methodology for decentralized cellular network optimization," 2016.

[19] C. Cox, *An Introduction to LTE: LTE, LTE-Advanced, SAE and 4G Mobile Communications*. Wiley, 2012.

[20] J. Zyren and W. McCoy, "Overview of the 3gpp long term evolution physical layer," *Freescale Semiconductor, Inc*, 2007.

[21] 3GPP, "E-UTRA: Physical Channels and Modulation," September 2009. TS 36.211, V12.7.0. Release 12 url: `http://www.3gpp.org/ftp/Specs/archive/36_series/36.211/36211-c70.zip`.

[22] S. Guruacharya, D. Niyato, D. I. Kim, and E. Hossain, "Hierarchical competition for downlink power allocation in ofdma femtocell networks," *IEEE Transactions on Wireless Communications*, vol. 12, pp. 1543–1553, April 2013.

[23] L. B. Le, D. Niyato, E. Hossain, D. I. Kim, and D. T. Hoang, "Qos-aware and energy-efficient resource management in ofdma femtocells," *IEEE Transactions on Wireless Communications*, vol. 12, pp. 180–194, January 2013.

[24] K. Zhu, E. Hossain, and A. Anpalagan, "Downlink power control in two-tier cellular ofdma networks under uncertainties: A robust stackelberg game," *IEEE Transactions on Communications*, vol. 63, pp. 520–535, Feb 2015.

[25] V. Chandrasekhar and J. Andrews, "Spectrum allocation in tiered cellular networks," *IEEE Transactions on Communications*, vol. 57, pp. 3059–3068, October 2009.

[26] C. Charalambous and N. Menemenlis, “Stochastic models for long-term multipath fading channels and their statistical properties,” in *Proceeding 38th IEEE Conference on Decision and Control*, vol. 5, pp. 4947–4952 vol.5, 1999.

[27] C. Charalambous and N. Menemenlis, “Stochastic models for short-term multipath fading channels: chi-square and ornstein-uhlenbeck processes,” in *Proceeding 38th IEEE Conference on Decision and Control*, vol. 5, pp. 4959–4964 vol.5, 1999.

[28] C. Charalambous and N. Menemenlis, “A state-space approach in modeling multipath fading channels via stochastic differential equations,” in *IEEE International Conference on Communications*, vol. 7, pp. 2251–2255 vol.7, 2001.

[29] S. D. Mohammed Olama and C. Charalambous, *Wireless Fading Channel Models: from Classical to Stochastic Differential Equations, Stochastic Control*. InTech, 2010.

[30] J. C. Cox, J. E, Ingersoll, and S. A. Ross, “A theory of the term structure of interest rates,” *Econometrica*, vol. 53, no. 2, pp. 385–407, 1985.

[31] W. Feller, “Two singular diffusion problems,” *Annals of Mathematics*, vol. 54, no. 1, pp. 173–182, 1951.

[32] R. Z. Khasminskii and G. Yin, “On transition densities of singularly perturbed diffusions with fast and slow components,” *SIAM Journal on Applied Mathematics*, vol. 56, no. 6, pp. 1794–1819, 1996.

[33] R. Khasminskii and G. Yin, “Limit behavior of two-time-scale diffusions revisited,” *Journal of Differential Equations*, vol. 212, no. 1, pp. 85 – 113, 2005.

[34] H. J. Kushner, *Weak convergence methods and singularly perturbed stochastic control and filtering problems*. Systems & control, Boston: Birkhuser, 1990.

[35] "Mobile Station-Base Station compatibility Standard for Dual-Mode Wideband Spread Spectrum Cellular System, TIA/EIA Interim Standard 95(IS-95-A), Washington, DC: Telecommunications Industry Association," May 1995.

[36] S. V. Hanly and D. Tse, "Power control and capacity of spread spectrum wireless networks," *Automatica*, vol. 35, p. pp., 1999.

[37] QUALCOMM Incorporated, "An overview of the application of code division multiple access (cdma) to digital cellular systems and personal cellular networks," 1992.

[38] L. C. Evans, *Partial differential equations.* Graduate studies in mathematics, Providence (R.I.): American Mathematical Society, 1998.

[39] J. Yong and X. Zhou, *Stochastic Controls: Hamiltonian Systems and HJB Equations.* Stochastic Modelling and Applied Probability, Springer New York, 2012.

[40] E. Tadmor, "A review of numerical methods for nonlinear partial differential equations," 2012.

[41] A. Bensoussan, J. Frehse, and P. Yam, *Mean Field Games and Mean Field Type Control Theory.* SpringerBriefs in Mathematics, Springer New York, 1 ed., 2013.